# 1-7.Copper biomineralization with banded structure at Dogamaru mine, Shimane Prefecture, Japan



# Copper biomineralization with banded structure at Dogamaru mine, Shimane Prefecture, Japan

Hiroaki Watanabe[1], Kazue Tazaki[2], ABM Rafiqul Islam[3] and S. Khodijah Chaerun[3]

[1]*354-2 Oshitate, Inagi, Tokyo 206-0811 Japan*

[2]*Department of Earth Sciences, Faculty of Science, Kanazawa University, Kakuma, Kanazawa, Ishikawa 920-1192 Japan*

[3]*Graduate School of Natural Science and Technology, Kanazawa University, Kakuma, Kanazawa, Ishikawa 920-1192 Japan*

## Abstract

Large amounts of copper (2.6 - 2.7 ppm) and zinc (28.1 - 29.5 ppm) ions were found in the drainage system enclosed to the pits of Dogamaru mine, Shimane Prefecture, Japan. Vivid green and blue biomats were mainly composed of filamentous cyanobacteria predominated in the drainage of the mine. These biomats were rich in copper and zinc as major elements in association with copper minerals. The XRD analysis of the biomats revealed that the predominant mineral compositions were woodwardite ($Cu_4A_{l2}(SO_4)(OH)_{12}$ · $2\text{-}4H_2O$), a minor amount of dioptase ($CuSiO_2(OH)_2$) and shattuckite ($Cu_5(SiO_3)_4(OH)_2$). The results were aggred to that of TEM observation confirmed by the electron diffraction pattern at 2.4 Å for woodwardite ($Cu_4A_{l2}(SO_4)(OH)_{12}$. The NCS, ED-XRF and EPMA analyses supported the presence of the elements and their distribution in relation to the mineral formation. Furthermore, optical and scanning electron microscopic observations also showed that the most of microorganisms were encrusted with copper minerals where the predominantly filamentous cyanobacteria contributed to copper mineralization and stromatolite-like structures. Additionally, microscopic observations and FT-IR analysis also confirmed that copper mineralization took place in the extra cellular sheath in which

was converted into a nucleus for woodwardite mineralization. The stromatolite-like banded structures consisted of the banded layers in mm order and the laminae textures in μm order. Basically, the banded structure formation occurred by the differences such as cyanobacterial growth direction, distribution and mineralogical crystallinity, whereas micro laminae one occurred in correlation with cyanobacterial cell sizes. These results obviously confirmed that copper-biomineralization and the formation of stromatolite-like banded structures were regulated by the cyanobacterial activity in biomats.

***Key words***: Biomats, Cyanobacteria, Biomineralization, Stromatolite, Banded structure, Woodwardite, Cu, Zn

## INTRODUCTION

Metallic ore deposits are distributed everywhere in the world, which accumulate the useful elements for the utilization of human beings. Specially, not only iron but also copper has been utilized widely from the ancient to the present times (Hata 1997). There are various types of copper ore deposits namely 1) orthomagmatic deposit, 2) hydrothermal deposit and 3) sedimentary deposit (Iiyama 1998). In the sedimentary copper deposit, White Pine (U.S.A.), Zambian Copperbelt, Redstone (Canada), red-bed copper deposits and Kupferschiefer (Preidl and Metzler 1984; Rose and Bianchi-Mosquera 1993) are known as stratiform copper deposit showing relations with stromatolites (Mendelsohn 1976; Nishioka et al. 1984; Haynes 1986).

There are some copper mines rich in cuprite, native copper and other different copper ores in Japan. Some of them are Ogoya and Sawaguchi in Ishikawa, Shirataki in Kochi and Fukiya in Okayama Prefecture, while Dogamaru mine in Shimane Prefecture is a typical one among them (Kishigami et al. 1999; Watanabe and Tazaki 1998a, 1998b, 1999, 2000). Besides this, the drainage of mining area is of great significance as they contribute in the environmental pollution. It is also reported that the rivers draining metal mine area are often seriously affected by acid run-off from mining pits and waste rock piles (Fowler and Crundwell 1998; Hudson-Edwards et al. 1999). The mining

drainage contains large amounts of heavy metals, which have toxicity in different extents. It is well established that the presence of heavy metals or metaloids such as Mn, Fe, Cu, Zn, Cd, and Pb or As in any water system have a serious impact on the aquatic or terrestrial animals including mammals (Tazaki et al. 2002). Furthermore, the use and dispersion of metals has increased vastly during $20^{th}$ century, and the behavior of metals in the environment is therefore a matter of rising concern (Ledin 2000). Generally, ore deposits contain metals and minerals as well. The mineral formation takes place not only by the inorganic processes but also by the contribution of microorganisms are reported (Mendelsohn 1976; Haynes 1986; Rose and Bianchi-Mosquera 1993). There are some experimental researches that have been carried out for copper tolerance, bioleaching and biomineralization in recent years (Little et al. 1997; Ledin 2000; Kishigami et al. 1999). However, they are of very few in numbers for Cu-rich biomats in nature or in copper mine, where Fe- and Fe-Cu sulfides also commonly occurred.

Recently, bioremediation and phytoremediation of heavy metals has attracted growing attention because of several problems in association with pollutant removal using conventional method. Bioremediation strategies have been proposed as an attractive alternative owing to their low cost and high efficiency (Wang et al. 1998; Mejáre and Bülow 2001). Biomineralization is one of the processes by which microorganisms accumulate metalic ion on/in to the microbial surface from the drainage and make them immobilize (Tazaki 1999). The balance between mobilization and immobilization of heavy metals varies depending on the organisms involved, their environment and physico-chemical conditions (Gadd 2002). In the very recent study of Kigishima et al. (1999), Watanabe and Tazaki (1998a, 1998b, 1999, 2000) suggested that copper - bearing biomats are of varieties in colour with different contents, some of them are Cu-rich, and others are Fe- or Fe-Cu sulfides rich in the nature or in copper mine. However, no one has focused on the specific microorgnisms where those are present in biomats and can play a great role in copper biomineralization.

In this paper, the micro-morphological, mineralogical, biological and chemical characteristics of biomats are described and these results were therefore used to elucidate the copper-biomineralization and stromatolite-like structure formation mechanisms by cyanobacteria occurred around the copper mining drainage.

## LOCATION AND GEOLOGY

Dogamaru mine is located at the district of Ouchi (35°N, 132°E) in Shimane Prefecture, Japan (Fig. 1). The history of this mine went back at least until 1400's, and it had been operated as the leading copper mine in San-in district in 1890's (Shimane Prefecture 1985). At present, this mine is closed but many pits, strip mining site and waste dump areas are preserved. The Late Cretaceous to Palaeogene volcanic rocks and intrusive rocks are distributed in this area. They are ryholitic pyroclastic rocks in Ouchi Group and rhyolitic to andesitic pyroclastic rocks and lava in Takayama Group. The intrusive rocks consist of granites, felsite, granodiorite and dacite (Research Group for the San' in Late Mesozoic Igneous Activity 1979; Matsuda and Oda 1982). Around the mine, ryholitic pyroclastic rocks of Ouchi Group and Ombara Granite intruded to Ouchi Group are distributed. The ore deposits are vein-type hosted in rhyolite and partly skarn containing hedenbergite and garnet. Various ore minerals have been found, such as native copper (Cu), chalcocite ($Cu_2S$), covellite (CuS), calcopyrite ($CuFeS_2$), pyrite ($FeS_2$), marcasite ($FeS_2$), pyrrhotite ($Fe_{1-x}S$), sphalerite (ZnS), galena (PbS), arsenopyrite (FeAsS), molybdenite ($MoS_2$), argentite ($Ag_2S$), azurite ($Cu_3(CO_3)_2(OH)_2$), cerussite ($PbCO_3$), Ni-Co-Te mineral, magnetite ($Fe_3O_4$) and cassiterite ($SnO_2$) (Shimane Prefecture 1985; Matsuda and Akasaka 1995).

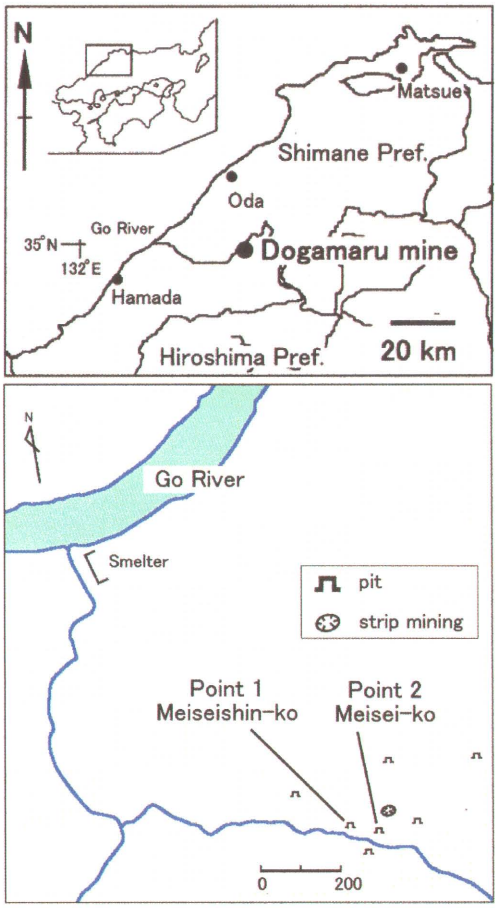


**Fig. 1** Location map of Dogamaru mine in Shimane Prefecture, Japan. Biomats occur at the Meiseishin-ko and Meisei-ko.

## SAMPLES

At Dogamaru mine, green and blue biomats have occurred profusely (Fig. 2). Green biomats formed at the pit named Meiseishin-ko (Point 1) (Fig. 2A). The drainage is flowing out from this pit therefore the cliff just before the entrance of pit that is converted into a waterfall about 10 m in height (Fig. 2A). A kind of moss thought to be "copper moss" (ex. *Scopelophila cataractae M.*) grow as thick as light brown to yellow-green colored biomats near the entrance of the pit along the flow. Green biomats

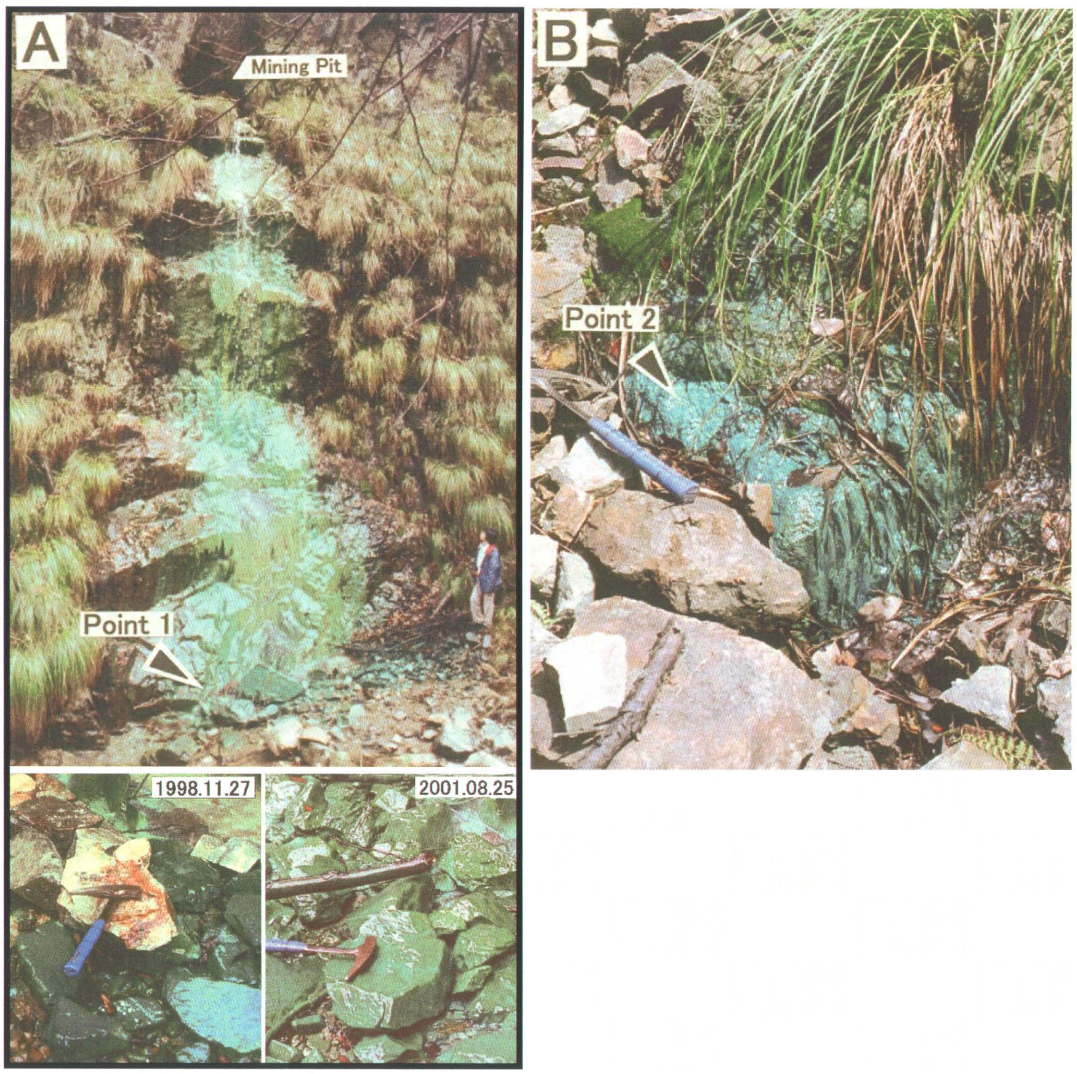


**Fig. 2** Occurrence of green (A) and blue (B) biomats at Dogamaru mine. Green biomats formed on the cliff, which is 10 meters in height from the mining pit, where gravels are covered with biomats beneath the cliff (A) (Point 1). The gravels that were uncovered with biomats were covered with green biomats of 0.7 mm in thickness for 33 months. Blue biomats occurred on the rock surface of the waste dump drainage area (B) (Point 2).

on the upper part of fall walls consists mainly of green algae where a thick film is produced. The lower part of fall walls and gravels at the beneath of cliff are covered with green biomats. In vertical section, the green biomats formed having crusts and fine band with thickness of about ~ 5 mm. Uncovered gravels have set up beneath the waterfall. It is found that they are covered with green biomats of 0.2 mm (in 12 months) and 0.7 mm (in 33 months) in thickness, which can be broken down easily by the fingertips.

Blue biomats are seen around the waste dump area before the pit named Meisei-ko (Point 2) (Fig. 2B), where it left Point 1 as long as 80 m (Fig. 1). They have covered the surface of waste rock and outcrop where exuding drainage are found available in this area. A kind of moss thought to be a "copper moss" grows there with blue biomats as well. Biomats that formed on the waste rock show blue surface (Fig. 2B), while at lower layer they are yellowish green in color. After picking up of blue biomats, they turn into dark green in color with blue tint within 1-2 days. After 1998, the vivid blue color has turned into the color where green tint is found stronger. They contain a lot of plant pieces. Besides this, blue biomats also formed on the outcrop. The whole of biomats are of blue in color as exception the part of those surfaces is covered with dark green biomats. In this research, green and blue biomats with drainage water were collected from point 1 and 2 of sampling area for investigation.

## METHODS

The following methods were applied for the investigation of afore mentioned biomats and drainage water samples.

### Water quality

To obtain data of drainage water quality of pH, Eh, EC and DO are measured in the field by using portable water quality inspection meters (pH; D-12, Eh; D-13, EC; ES-12, DO; OM-12 made by HORIBA). Considering the seasonal variations, the measurements were carried out for 12 times continuously from the August 14$^{th}$ 1997 to November 27$^{th}$ 1998. In addition, Fe, Cu and Zn contents in water were also quantified with the atomic absorption analyses (Seiko SAS-727) after filtrated through the 0.45 μm pore filter.

### Determination of Chemical compositions in Biomats

Bulk chemical compositions of biomats were analyzed by Energy dispersive X-ray fluorescence (ED-XRF) spectroscopy. Air-dried powdered biomats samples of Dogamaru mine were taken on to the miler film for analysis. The analysis was carried out by JEOL JSX 3201 using Rh K $\alpha$ radiation at an accelerating voltage of 30 kV under the vacuum condition. Biomats were divided into two portions, the surface and the bottom for analysis to quantify the total contents of carbon and nitrogen. The NCS elemental analyzer (AMUKO NA2500) was used to conduct the analysis.

### X-ray powder diffractometric analysis (XRD)

The minerological identification of biomats was determined by the X-ray powder diffractometer (XRD; Rigaku RINT2000). The analysis was carried out with Cu K $\alpha$ radiation at 40 kV and 30 mA. Biomats were analyzed as unoriented sample after air-drying. Furthermore, heat-dried samples were analyzed. Heating were ranged from 30 to 120 ℃ at intervals of about 30 ℃ per hour.

### Fourier-Transform Infrared absorbance spectroscopy (FT-IR)

Biomats were examined by using fourier transform infrared absorbance spectroscopy (Jasco FT/IR-610, MICR0-20). A drop of each cell suspension was mounted on a fluorite disk ($CaF_2$, 0.5 mm thick) for FT-IR analysis. After air-drying, cells were selected under the IR microscope.

### Optical microscopy

To identify the presence and variety of microbes, optical microscopic observation was carried out. Wet biomats were mounted on slide glasses and observed for the microorganism associated with the mineral by differential interference microscope (Nikon NTF2). Biomats were also inspected under episcopic fluorescence microscope (Nikon EFD3) in order to confirm the presence of chlorophyll and living state of microorganisms. After staining with 4'6-diamidino-2-phenylindole (DAPI), autofluorescence and fluorescence from microbes and minerals were observed. The vertical sections of biomats strengthened the cyanoacryate-bond after the air-drying polished thin sections were also observed with polarized and ore microscope (Nikon OPTIPHOT2-POL).

## SEM-EDX observation and analysis

The scanning electron microscope equipped with an energy dispersive X-ray spectroscopy (SEM-EDX; SEM: JEOL JSM-5200LV and EDX: PHILLIPS EDAX PV9800EX) was undertaken in order to observe the micro morphological structures of microbes in biomats and its association with some particles which include some elements. Fine structures of biomats were observed by the secondary and back-scattered electron images (SEI and BEI) of SEM. To observe the vertical section, handpicked biomats were fixed on the sample holder and cut them perpendicularly with the razor. Dehhdrated samples were coated with C, Au or Os for observation and analysis. The observations were carried out in 15 kV with different magnifications. Os-coating was trusted to Japan Laser co. LTD and Meiwa Shoji co. LTD. Chemical compositions of the micro-area of the sample were analyzed by energy dispersive X-ray spectrometer (EDX) equipped with the SEM at the accelerating voltage of 15 and 20 kV.

## Transmission electron microscopy (TEM)

Techniques of transmission electron microscopy (TEM; JEOL JEM-2000EX) were used for the observation of extra cellular images of microorganisms. This was also equipped with electron diffraction (ED) analysis, which can identify minerals through the diffraction pattern of biomats. One drop of the suspension of biomats and other drop of drainage water were mounted on the separate micro grids. After air-drying, the uncoated samples were observed and analysed at an accelerating voltage of 120 kV.

## Electron probe microanalysis of biomats (EPMA)

Complimentary techniques of electron probe microanalyzer (EPMA, JEOL JXA-8800R) were carried out for the quantitative analyses of biomats. The C or Au coated polished thin sections of biomats were analysed to identify the element distribution in them. Mainly X-ray mappings for C, S, Al, Si, Cu and Zn were carried out with the EPMA. The quantitative analyses were carried out at the accelerating voltage of 15kV, with probe current $5.0 \times 10^{-9}$ A and probe diameter "0".

# RESULTS

## Characteristics of water and biomats at Dogamaru mine

### Water quality of the drainage water at point 1 and 2

Chemical characteristics of the drainage water at Point 1 and 2 were measured continuously from year 1997 to 1999 with various intervals. Chemical characteristics of the tributary of Go River were also measured from year 1997 to 1998 (Table 1). As this tributary run in the mining area and seemed to have a few influences on the mining drainage, measurements were undertaken at the upstream. Field measurements of the drainage water, pH ranged from 6.0 to 6.6, electrode potential vs. standard hydrogen electrode (Eh) ranged from 207 to 338 mV, electrical conductivity (EC) ranged from 0.31 to 0.45 mS/cm, dissolved oxygen (DO) ranged from 5.4 to 8.2 mg/l and temperature ranged from 12 to 13 ℃. Whereas, in the tributary of Go River, pH was about 7.0, Eh was 190 ~ 284 mV, and EC was 0.07 ~ 0.09 mS/cm. An exception was found on measurement of November 27, 1998, which showed EC was 0.26 mS/cm and DO was 6.8 ~ 9.5 mg/l. Remarkably, EC values in drainage water showed 4 to 5 times higher than that of the river water. Atomic absorption analyses (AAS) of drainage water showed that the Cu concentrations at point 1 and 2 were 2.59 ppm and 2.65 ppm, whereas Zn concentrations were 28.06 and 29.51 ppm, respectively, measured on April 27, 1998 (Table 1).

**Table 1** Physical properties and atomic absorption analysis of water collected from mining drainage, and NC analyses of biomats.

| | | Water chemistry | | | | | | | | Biomats (wt. %) | | |
|---|---|---|---|---|---|---|---|---|---|---|---|---|
| | | pH | Eh (mV) | EC (mS/cm) | DO (mg/l) | WT (℃) | atomic absorption (ppm) | | | Portion | N | C |
| | | | | | | | Fe | Cu | Zn | | | |
| Point 1 | 1997.08.14 | 6.4 | 310 | 0.31 | 5.9 | 13.2 | 0.02 | 2.59 | 28.06 | surface | 0.21 | 2.95 |
| | 1998.04.27 | 6.5 | 240 | 0.40 | 5.4 | 13.4 | | | | | | |
| | 1998.07.30 | 6.5 | 243 | 0.37 | 8.2 | — | | | | bottom | 0.16 | 1.86 |
| | 1998.11.27 | 6.0 | 338 | 0.45 | 6.6 | 12.4 | | | | | | |
| | 1999.04.04 | 6.4 | 213 | 0.41 | 6.6 | 12.4 | | | | | | |
| Point 2 | 1997.08.14 | 6.3 | 276 | 0.38 | 5.4 | — | 0.01 | 2.65 | 29.51 | surface | 0.26 | 2.87 |
| | 1998.04.27 | 6.6 | 293 | 0.41 | 7.7 | — | | | | bottom | 0.23 | 2.42 |
| | 1999.04.04 | 6.3 | 256 | 0.41 | 5.8 | 12.3 | | | | | | |
| Go River | 1997.08.14 | 6.8 | 237 | 0.07 | 6.8 | 20.8 | - | - | - | - | - | - |
| | 1998.04.27 | 7.3 | 207 | 0.09 | 7.6 | 13.9 | | | | | | |
| | 1998.07.30 | 7.2 | 192 | 0.08 | 8.2 | — | | | | | | |
| | 1998.11.27 | 7.2 | 284 | 0.26 | 9.5 | 10.5 | | | | | | |

- ; not detected

## Green biomats of Meiseishin-ko (Point 1)

### Chemical compositions of green biomats

Chemical compositions of green biomats were determined by using ED-XRF and NCS analyzers. ED-XRF analysis showed that green biomats contained large amounts of Cu and Zn with traces of Al, Si, S, Ca, Fe and Pb (Fig. 3). Zn content was lower than that of Cu in the green biomats. Whereas the NCS elemental analysis showed that carbon contents in surface (cortical layer) and bottom (lower layer) of the biomats were 2.95 wt% and 1.86 wt%, respectively, while the nitrogen contents were 0.21 wt% in the surface and 0.16 wt% in the bottom of the green biomats (Table 1). The contents of carbon and nitrogen in cortical layers were higher than that of the lower layers. Conversely, AAS analysis of drainage water elucidated that Zn concentration was higher than that of Cu (Table 1).

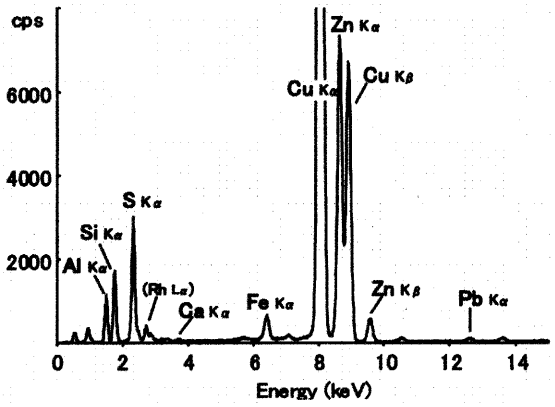


**Fig. 3** ED-XRF analysis of green biomats showing the presence of large amounts of Cu and Zn with traces of Al, Si, S, Ca, Fe and Pb.

XRD analyses of green biomats

XRD pattern of green biomats showed the broad reflections at 10.6 Å (100), 5.3 Å (34), 3.6 Å (31), 2.6 Å (41) and 1.5 Å (27) (Fig. 4A) which was similar to that of "Caernarvonshire woodwardite" (10.9 (100), 5.46 (60), 3.66 (50), 2.613 (40), 2.454 (20), 1.535 (5): JCPDS card No. 39-0726). Even there is no reflection of such elements (Si, Ca, Fe, Zn and Pb) analyzed by ED-XRF as primary components of mineral formation. XRD analyses were carried out to examine the stability of green biomats at temperatures of 30 ~ 120 ℃ with interval of 30 ℃ (Fig. 4B). A basal spacing of woodwardite in green biomats decreased progressively to 8.09 Å at 120 ℃, and intensity fell down rapidly at 90 ℃. The reflections almost disappeared at 90 ℃, while the reflections of 5.15 and 3.62 Å changed into 4.10 Å at 60 ℃ and disappeared at

90 ℃. Moreover, the reflection of 2.61 Å was almost constant, even though its intensity fell down rapidly at 90 ℃.

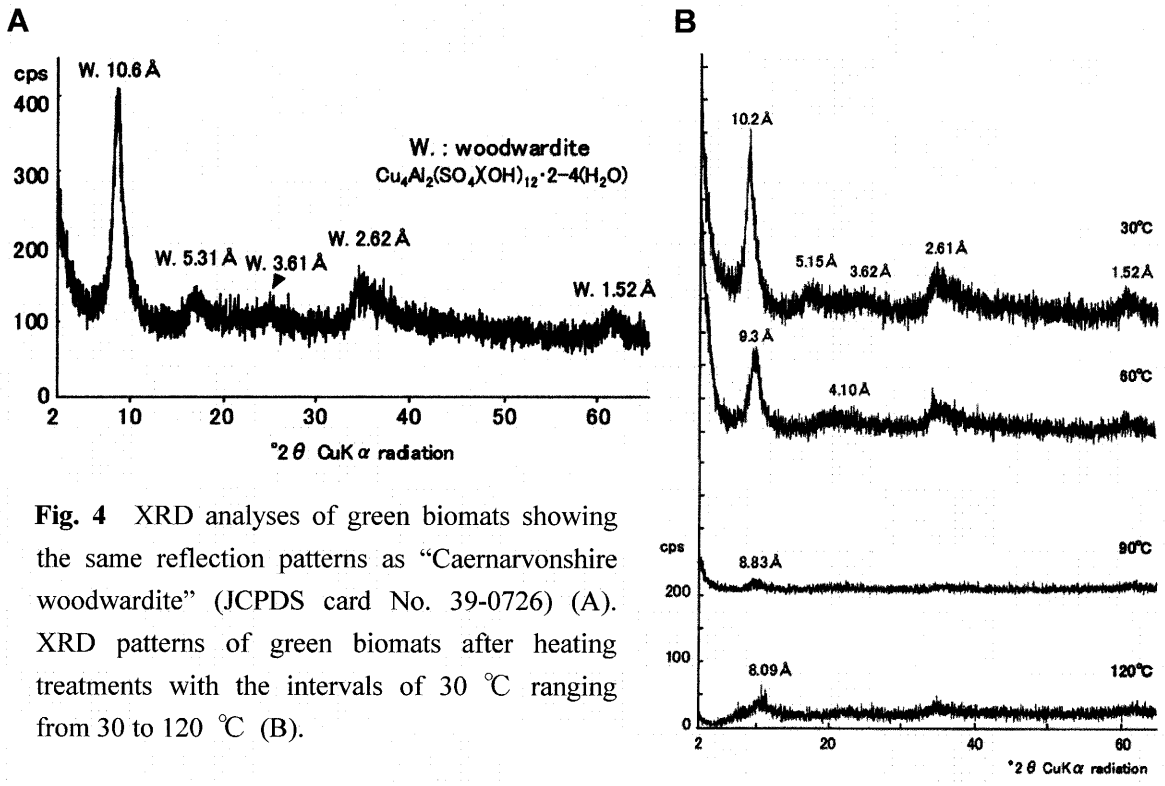


**Fig. 4** XRD analyses of green biomats showing the same reflection patterns as "Caernarvonshire woodwardite" (JCPDS card No. 39-0726) (A). XRD patterns of green biomats after heating treatments with the intervals of 30 ℃ ranging from 30 to 120 ℃ (B).

## FT-IR spectroscopy of green biomats

IR spectrum of green biomats indicated the presence of organic substance in its grain, showing the bands at 3700-3100 $cm^{-1}$ (O-H stretch), 3285 $cm^{-1}$ (N-H stretch), 2922 $cm^{-1}$ (C-H stretch), 1655 $cm^{-1}$ (C=O stretch), 1545 $cm^{-1}$ (C-N-H stretch) and 1399 $cm^{-1}$ (C-H stretch) (Fig. 5). The N-H, C=O and C-N-H bands were derived from peptides in microbial cells of green biomats.

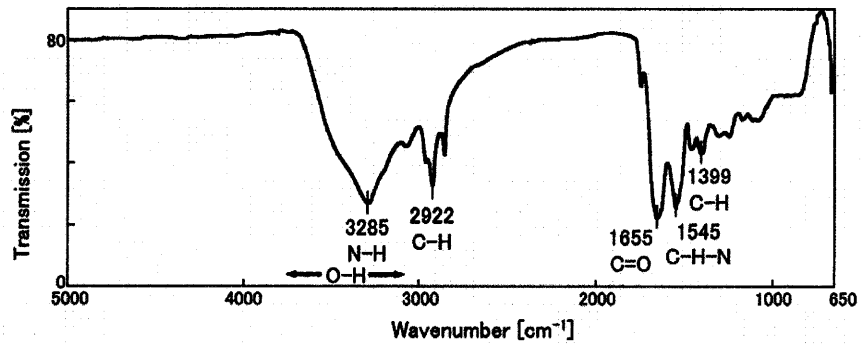


**Fig. 5** FT-IR spectrum of green biomats indicating the presence of organic substance in the grain, showing 3700-3100 $cm^{-1}$ (O-H stretch), 3285 $cm^{-1}$ (N-H stretch), 2922 $cm^{-1}$ (C-H stretch), 1655 $cm^{-1}$ (C=O stretch), 1545 $cm^{-1}$ (C-N-H stretch) and 1399 $cm^{-1}$ (C-H stretch).

**Optical microscopic observation of green biomats**

Biomats were observed with differential interference and episcopic fluorescence microscope. The tabular, columnar, domal and spherical grains which were of translucent, green or sometimes brown in color were observed in the green biomats (Fig. 6). These showed a stromatolite-like micro banding. DAPI-stained samples displayed red and blue fluorescence under the ultraviolet ray that confirmed the presence of chlorophyll and DNA respectively, (Fig. 6B, D) indicating the presence of living microorganisms such as cyanobacteria, rod-shaped bacteria, coccus, hyphomycetes and green algae.

These were adhered with fine granules, and covered with crystalline sheath. In particular, cyanobacteria were among the predominant and characteristic microorganisms in the green biomats. The teardrop-shaped sheath forming on the tips of cyanobacteria was also characteristic in the green biomats (Fig. 6A, B). The sheath of the same type was recognized on the green algae too. They showed the concentric micro banding textures and were converted into nucleation site for ions dissolved in drainage water. Cyanobacterial cell was 1 to 2 μm in diameter and 2 to 10 μm (generally, 3 to 4 μm) in length. They formed filament on the microlaminae. Non-filamentous rod-shaped cyanobacteria were also recognized. The red fluorescence of chlorophyll and blue fluorescence of DNA for non-sheathed filaments were distinct, while sheathed ones were often weak or not detected. Similar to polarization-microscopic observations, it was found that there was a small amount of sheathed cyanobacteria in the green biomats formed newly and filamentous microorganisms grew along the domal particles boundary (Fig. 6C, D).

Furthermore, thin sections of green biomats were observed with polarization-microscope, showing stromatolite-like banded structures (Fig. 7). Millimeter-order bands including micro laminae was recognized in biomats. Pale green to transparency crystalline layer and green low-crystalline to amorphous layer appeared alternatively (Fig. 7A, B), while domal to columnar structure developed in the crystalline layer. A unit of banded structure ranging from 0.2 to 0.4 mm in width was constructed in a set of crystalline layer and low-crystalline to amorphous layer. Green biomats were also built with some units. The gravels that were not covered with biomats

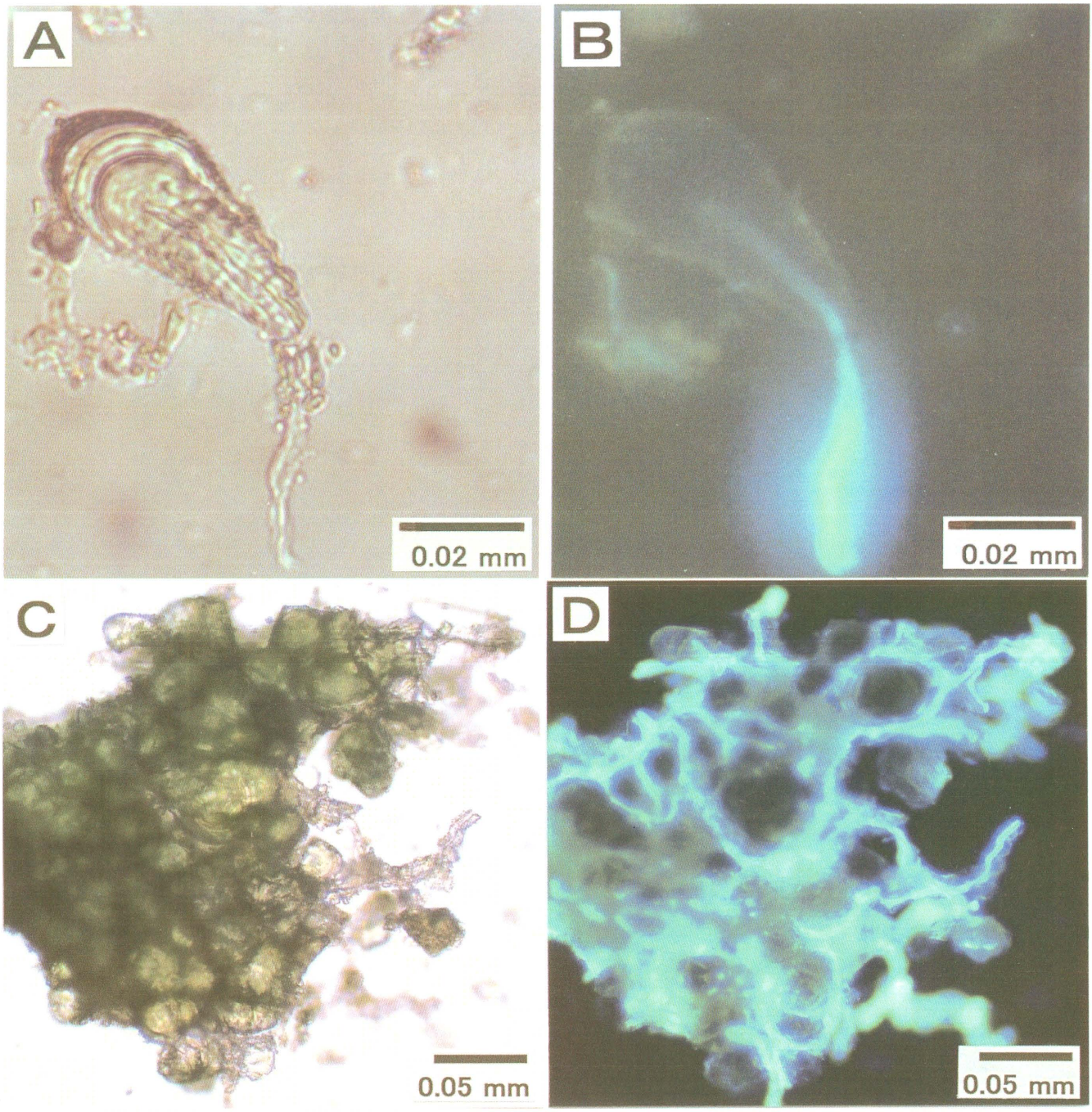


**Fig. 6** Differential interference (A, B) and fluorescence microscopic (B, D) images of green biomats. Teardrop-shaped sheath forming on the tip of cyanobacteria is characteristic in green biomats (A, B). Sheath shows a concentric micro laminae and filamentous microorganisms growing along the domal cells boundary (C, D).

were set up at beneath the waterfall. First, surface of gravels was covered with low-crystalline to amorphous layer. Next, crystalline layer was formed. Finally, one unit formed in 12 months and 2 or 3 units in 33 months. Woodwardite was identified with XRD. Under the microscope, it appeared to be transparent to pale green. Pleochroism was not found in this mineral. In the thin sections, an enormous number of filamentous microorganisms were recognized (Fig. 7C, D). Based on the morphological views and episcopic fluorescence microscopic observations, these were grouped as cyanobacteria. Numerous cyanobacteria grew toward to the surface of biomats (Fig. 7C), although some of them grew horizontally as parallel to the bands (Fig. 7D). The tip of the cyanobacterial filaments was covered with teardrop-shaped sheath showing concentric lamination (Fig. 7C).

Sometimes, sheath with the same type was recognized on the green algae. Sheath developed toward the growth direction of cyanobacteria. Basically, the teardrop-shaped sheath was formed on each of the cyanobacterial filaments. Gradual-development of concentric lamination was found over the sheath (Fig. 7C, D). The layered structure was constructed by repeated deposition of domal to columnar structures that were horizontally arranged. In the lower part of biomats, traces of the large microorganism, for instance, green algae were often found, while traces of cyanobacteria were little. Cyanobacterial growth in parallel towards the lamination was recognized (Fig. 7D). Lengthwise growth of cyanobacterial cells that was 0.2 mm in size was also observed in the thin section. In these cases, the width of each lamina corresponded to the diameter of the cyanobacteria. Cyanobacteria growing in parallel towards the lamination changed the growth direction to the biomats surface en route. As a result, the teardrop-shaped sheath was formed on the tip of cyanobacterial filament (red arrow in Fig. 7D). The rod-shaped bacteria formed colonies in parallel towards the banding were occasionally recognized.

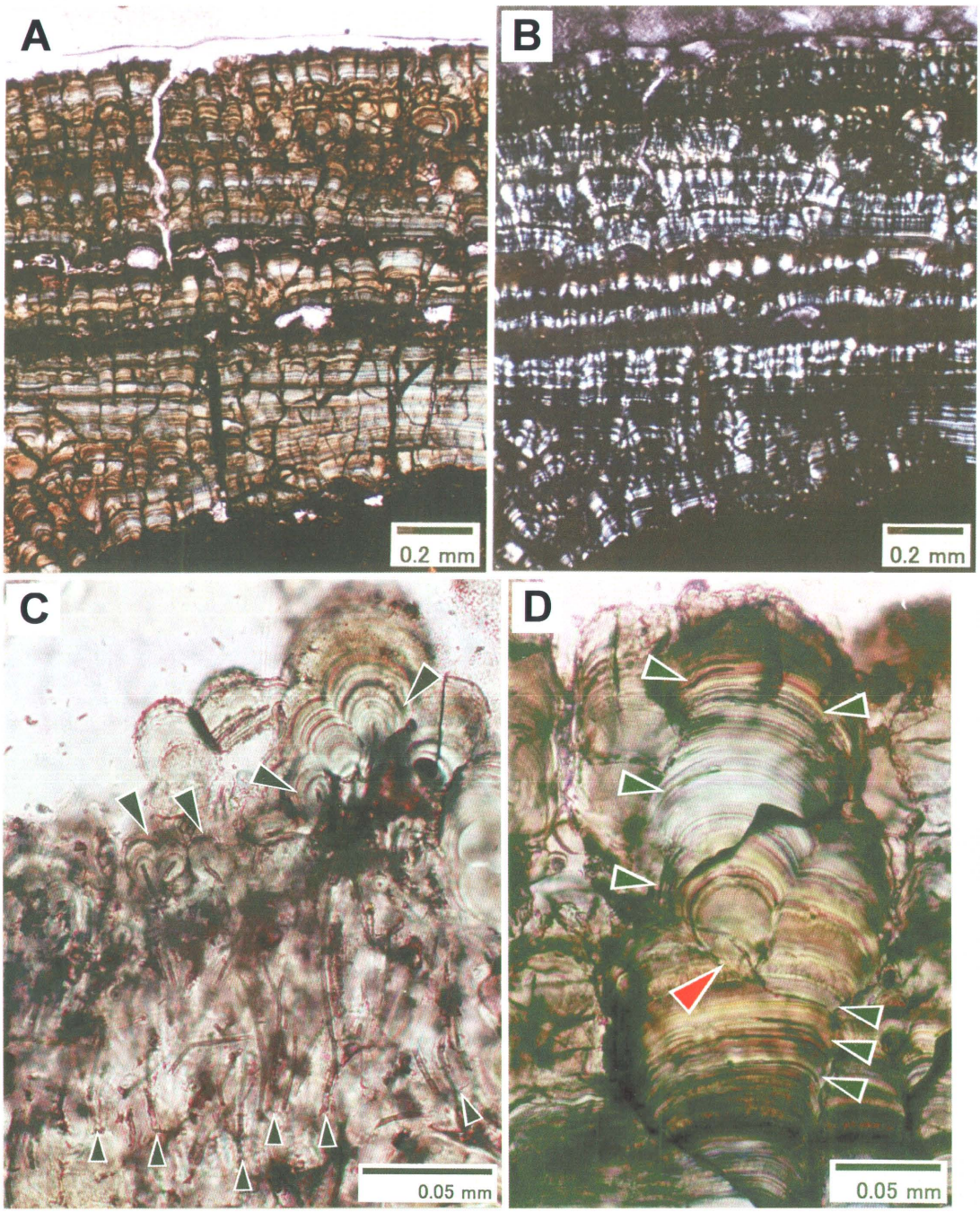


**Fig. 7** Polarization-microscopic images of green biomats showing stromatolite-like bands in the thin section (A: open polar, B: cross polar). Micron and millimeter order bands are recognized in biomats. Cyanobacteria grow towards the surface of biomats (small arrows in Fig. 7C). The tips of the cyanobacterial filaments are covered with teardrop-shaped sheath (large arrows in Fig. 7C). One teardrop-shaped sheath is formed on each of the cyanobacterial filaments. In the domal structure, cyanobacteria grow parallel to the lamination (arrows in Fig. 7D). In this case, width of each lamina corresponds to the diameter of the cyanobacteria. Teardrop-shaped sheath is shown (red arrow in Fig. 7D).

**SEM observations of green biomats**

The domal structures developing dense layer and cyanobacteria-rich porous layers were recognized (Fig. 8A). The dense layer corresponded to crystalline layer, whereas porous layer corresponded to low-crystalline to amorphous layer in the optical microscopic observation (see Fig. 7A, B). BEI images revealed the compositional concentric lamination in the sectioned biomats (Fig. 8B, C). The width of these bands ranged from 0.2 to 5 μm, while 30 to 40 laminae were also recognized in the layer of 50 μm thick. Some layers arranged domal to columnar structures showing lamination (Fig. 8C). The laminae in each column ran continuously. The dark circles of sectioned cyanobacteria were also found in the boundary of the columns (Fig. 8C). These diameters were adjusted to the width of lamina. In the biomats, there were cyanobacteria, green algae, spherical microorganisms and organic substances in association with inorganic matters. It was also found that particles adhered on cyanobacterial cells.

Finally, the teardrop-shaped sheath formed on the tip of cyanobacterial filament was characteristic (Fig. 9A). Moreover, sheaths showed the rough surface with fine grains and flakes, however cyanobacteria possessed the comparatively smooth and node surfaces. The domal to columnar structure was also formed on the sheath as a center.

In addition to elemental microanalyses of the biomats, EDX analyses also confirmed that sheath and grain in biomats consisted mainly of Al, Si, S, Cu, and Zn with the trace amount of Fe (Fig. 9B). The similar result was also found in the bulk analysis with ED-XRF (see Fig. 3), where the peak of Cu was higher than that of Zn. In observations of vertically sectioned sample, cyanobacterial filaments were also found in the sections of teardrop-shaped sheaths and domes (Fig. 10). Therefore, cyanobacterial filament consisted of cells that were about 2 μm in diameter and 1 to 2 or 3 to 4 μm in length. On the section, the concentric lines which were about 0.4 μm in width, were recognized in the intervals same as the joints of cells. Lamination span in relation to the length of the cells forming cyanobacterial filaments was also found in the sheath.

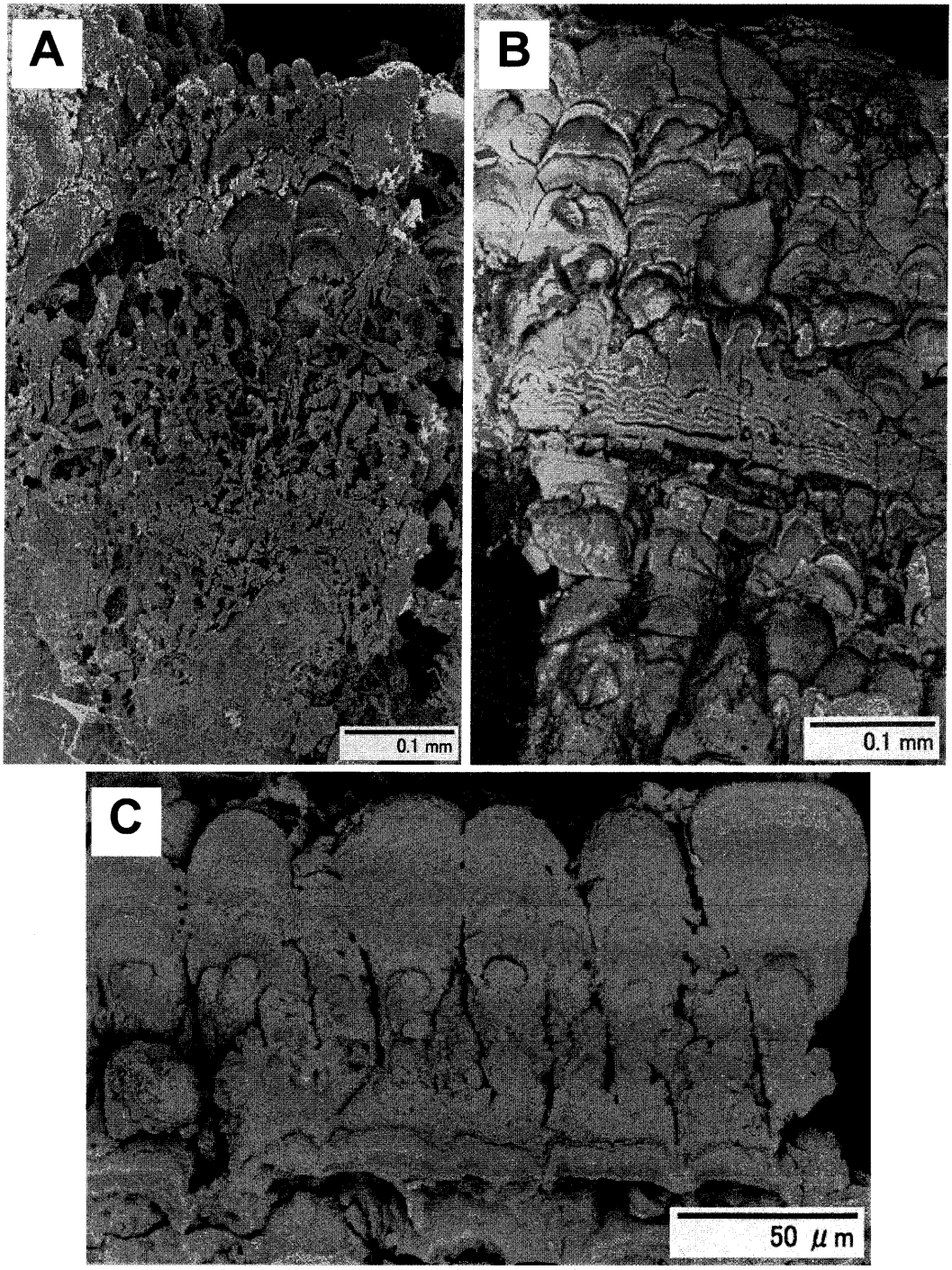


**Fig. 8** SEM images of green biomats showing the secondery electron image of green biomats (A). The layer developing the domal structures and cyanobacteria-rich porous layer are recognized. The arrangement of the teardrop-shaped sheaths is shown on the surface of biomats. Back-scattered electron images (BEI) of vertical sections (B, C), are visible.

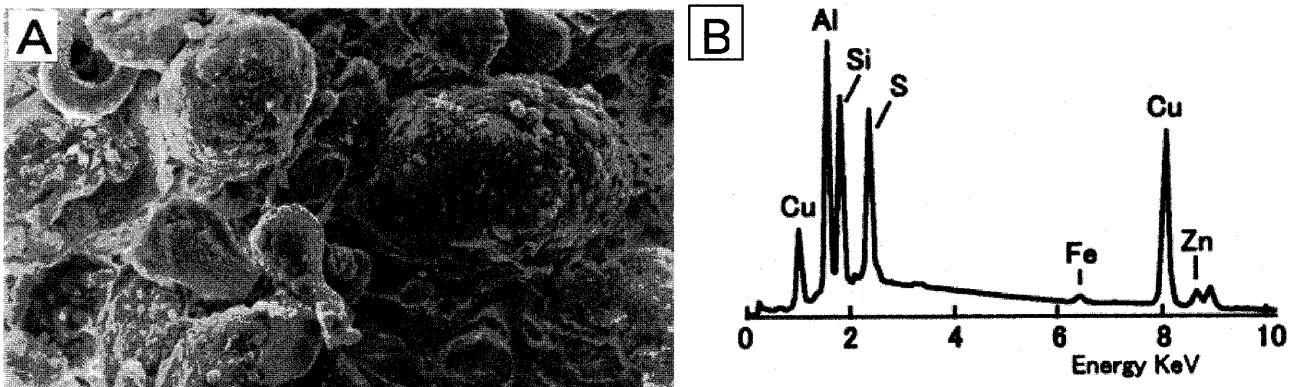


**Fig. 9** Secondery electron images (A) and EDX spectrum (B) of green biomats showing the teardrop-shaped sheath and numerous filamentous cyanobacteria. Sheaths aggregate together with cyanobacteria and other grains. Sheaths consist mainly of Al, Si, S, Cu and Zn with the trace of Fe (B).

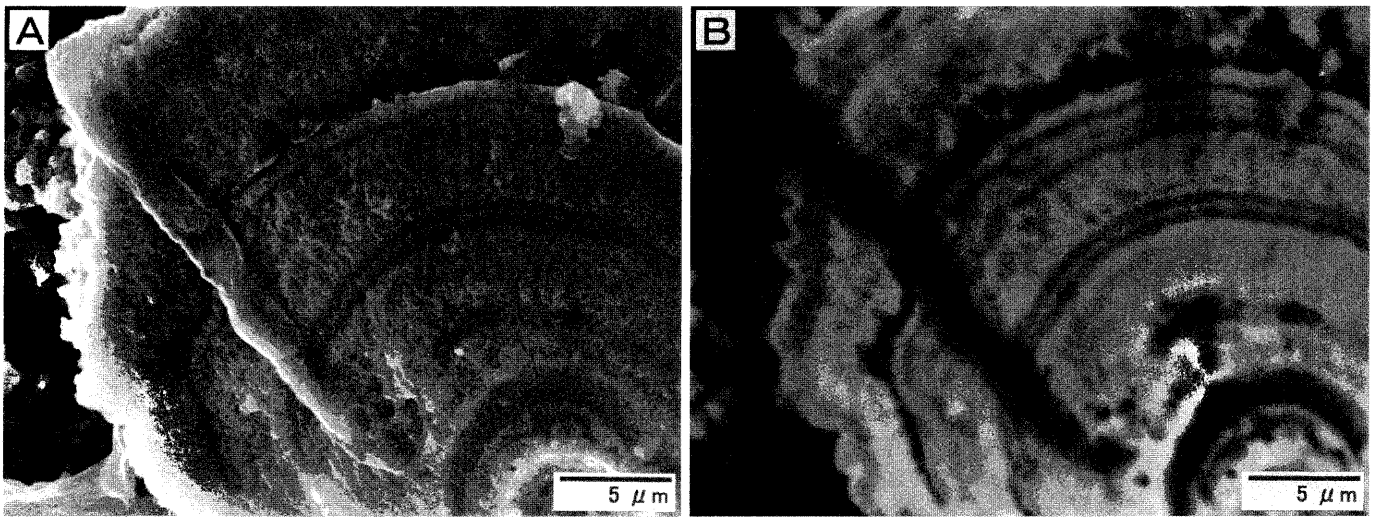


**Fig. 10** SEM images of green biomats in sectioned sample recognize the lamina span corresponding to the length of the cells consisting of cyanobacterial filament (A: SEI, B: BEI).

**TEM observation of green biomats**

Filamentous cyanobacteria that had thick extracellular sheath were observed with TEM (Fig. 11). The sheath extended before the tip of the filament. Many grains were attached on the sheath. Electron diffraction pattern of these grains showed 2.4 Å corresponding to d (015) of woodwardite (Fig. 4A). The bacilli attached grains were also recognized (Fig. 11: arrows).

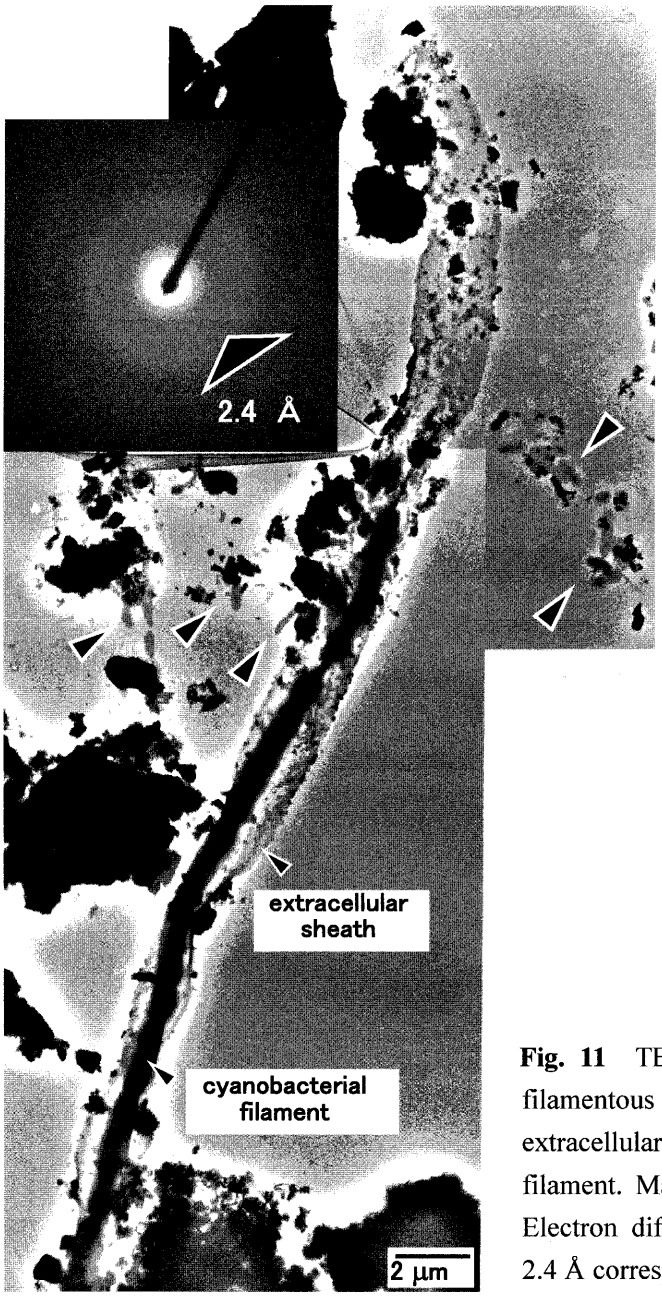


In addition, fine particles (Fig. 12A: small arrows) were recognized on the cellular surface and extracellular sheath of cyanobacteria (Fig. 12A: large arrow). Sheathed and non-sheathed bacilli were found on cyanobacterial filaments (Fig. 12B: arrows). It also seemed that bacilli were covered with flakes or encrusted with high dense materials. Flaky materials were formed on the cellular surface and around the cell (Fig. 12A-C). The lattice image was found in flaky materials where the lattice dimension was 10.4 Å (Fig. 12D). This value almost corresponded to basal spacing of woodwardite in green biomats. Polygonal plate-like particles were also found on cyanobacterial surface.

**Fig. 11** TEM images of green biomats showing filamentous cyanobacteria possesses thick extracellular sheath that extends before the tip of the filament. Many grains are attached on the sheath. Electron diffraction pattern of these grains shows 2.4 Å corresponding to d (015) of woodwardite. The bacilli attached grains are also recognized (arrows).

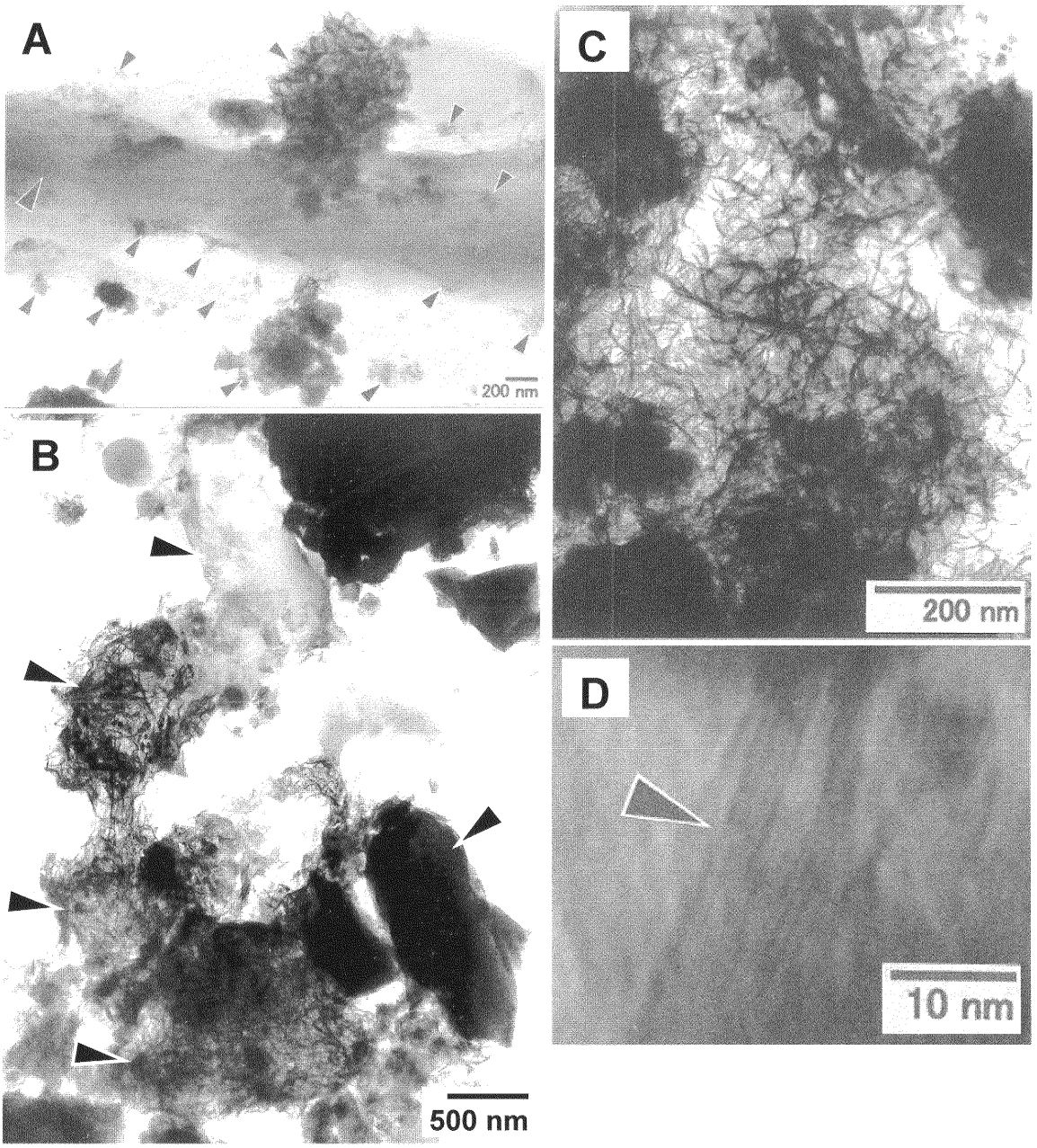


**Fig. 12** TEM images of green biomats showing cyanobacteria in close-up of Fig. 11 (A). Fine particles (small arrows in Fig. 12A) are recognized on the cellular surface and extracellular sheath of cyanobacteria (large arrow in Fig. 12A). Flaky materials are formed on the cellular surface. Sheathed and non-sheathed bacilli are found on cyanobacterial filament (B). Close-up images of flaky grains (C, D). The lattice image is also found with dimension of 10.4 Å. This value almost corresponds to basal spacing of woodwardite in green biomats.

**EPMA analyses of green biomats**

Whole parts of green biomats contained Al, Si, S, Cu and Zn. EPMA elemental mapping of C, S, Al, Si, Cu and Zn revealed banded elemental distributions. It clearly seemed that there were tendencies where Cu, Zn, Al and S contents were high at the light bands in BEI (Fig. 13, 14) suggesting components of woodwardite (Cu, Al, and S), and Zn might be the substitution of Cu. Carbon and Si were high concentration at the dark bands (Fig. 14). The sheaths formed at the tips of cyanobacterial filaments were also rich in carbon (arrows in Fig. 14 composition image).

Furthermore, quantitative analysis results are given in Table 2. The light bands in BEI contained 34 ~ 39 wt% CuO, 5 ~ 6 wt% ZnO, 16 ~ 19 wt% $Al_2O_3$, 8 ~ 12 wt% $SO_3$, 6 ~ 12 wt. % $SiO_2$ and trace amounts of FeO and PbO. While the dark bands in BEI were composed of 24 ~ 27 wt% CuO, 5 wt% ZnO, 21 ~ 24 wt% $Al_2O_3$, 7 ~ 8 wt% $SO_3$, 11 ~ 12 wt% $SiO_2$ and trace amounts of FeO and PbO. The light bands were richer in CuO and $SO_3$, and less in $Al_2O_3$ than those of dark bands. The low total weight percentages were significant interlayer and constitution of water and organics.

Raada (1985) has reported that Caernarvonshire 'woodwardite' contained 34.48 wt% CuO, 0.30 wt% ZnO, and 16.5 wt% $Al_2O_3$ ($SO_4$ was not analyzed). Besides that, Witzke (1999) also reported that hydrowoodwardite was composed of 28.39 wt% CuO, 0.41 wt% ZnO, 19.20 wt% $Al_2O_3$, 15.15 wt% $SO_4$, 30.10 wt% $H_2O$, 5.60 wt% $SiO_2$, and 0.10 wt% $Na_2O$. The light bands are rich in CuO and $SO_3$, and less in $Al_2O_3$ to compare with dark bands. Green biomats is rich in Al more than blue biomats whereas Cu is poor, showing low Cu/Al ratio (Table 2).

**Table 2** Electron microprobe analyses of green biomats. The low total wt% is due to adsorptive and crystallin water.

| | light parts (woodwardite) | | | | | dark parts | |
|---|---|---|---|---|---|---|---|
| FeO | 0.58 | 0.36 | — | — | — | 0.42 | 0.48 |
| CuO | 38.59 | 37.89 | 37.88 | 36.87 | 33.70 | 27.32 | 24.14 |
| ZnO | 5.81 | 5.35 | 5.56 | 5.80 | 5.92 | 5.42 | 4.71 |
| PbO | 0.13 | 0.18 | — | — | — | 0.72 | 0.72 |
| Al2O3 | 16.61 | 18.40 | 16.25 | 17.80 | 19.48 | 20.75 | 23.86 |
| SO3 | 9.80 | 11.60 | 10.42 | 11.31 | 8.49 | 8.21 | 6.83 |
| SiO2 | 8.97 | 5.81 | 8.50 | 6.49 | 11.91 | 11.40 | 11.57 |
| Total | 80.50 | 79.60 | 78.60 | 78.26 | 79.50 | 74.24 | 72.30 |
| | Cations per 10 oxygens calculated except for silica | | | | | | |
| Fe | 0.057 | 0.033 | — | — | — | 0.041 | 0.050 |
| Cu | 3.413 | 3.126 | 3.370 | 3.128 | 3.053 | 2.431 | 2.284 |
| Zn | 0.502 | 0.432 | 0.483 | 0.481 | 0.524 | 0.472 | 0.435 |
| Pb | 0.004 | 0.005 | — | — | — | 0.023 | 0.024 |
| Σ | 3.977 | 3.596 | 3.854 | 3.608 | 3.577 | 2.967 | 2.793 |
| Al | 2.292 | 2.369 | 2.256 | 2.355 | 2.754 | 2.881 | 3.521 |
| S | 0.862 | 0.950 | 0.921 | 0.953 | 0.764 | 0.726 | 0.642 |
| Si | — | — | — | — | — | — | — |
| Total | 7.131 | 6.915 | 7.030 | 6.917 | 7.095 | 6.574 | 6.956 |
| | | | | | | Total Fe as FeO | |

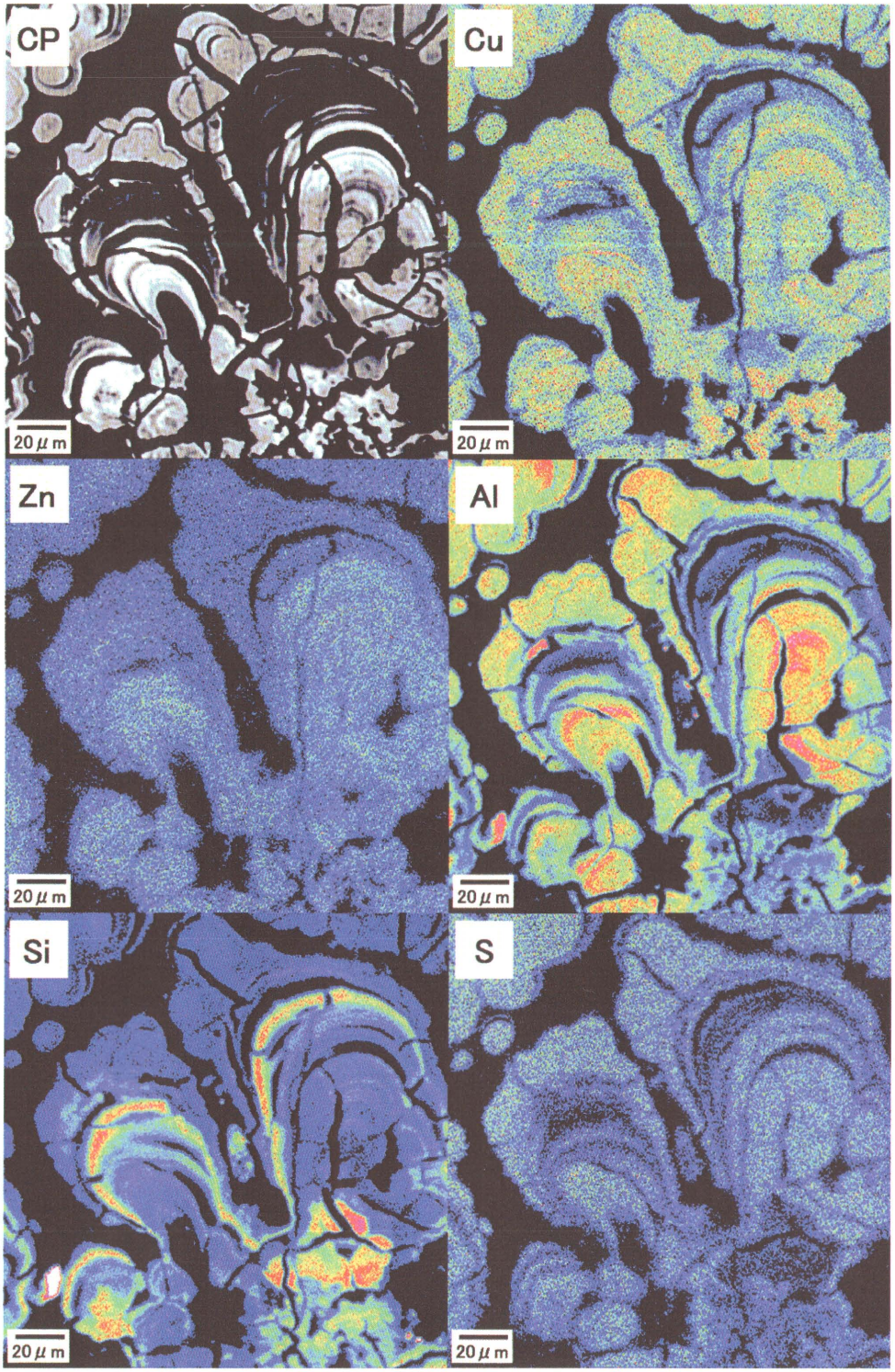


**Fig. 13** EPMA color mapping of green biomats reveals banded elemental distributions. There is tendency that Cu, Zn, Al and S contents are high at the light bands in BEI. Cu, Al and S are components of woodwardite, and Zn may be the substitution of Cu, while Si is high at the dark bands.

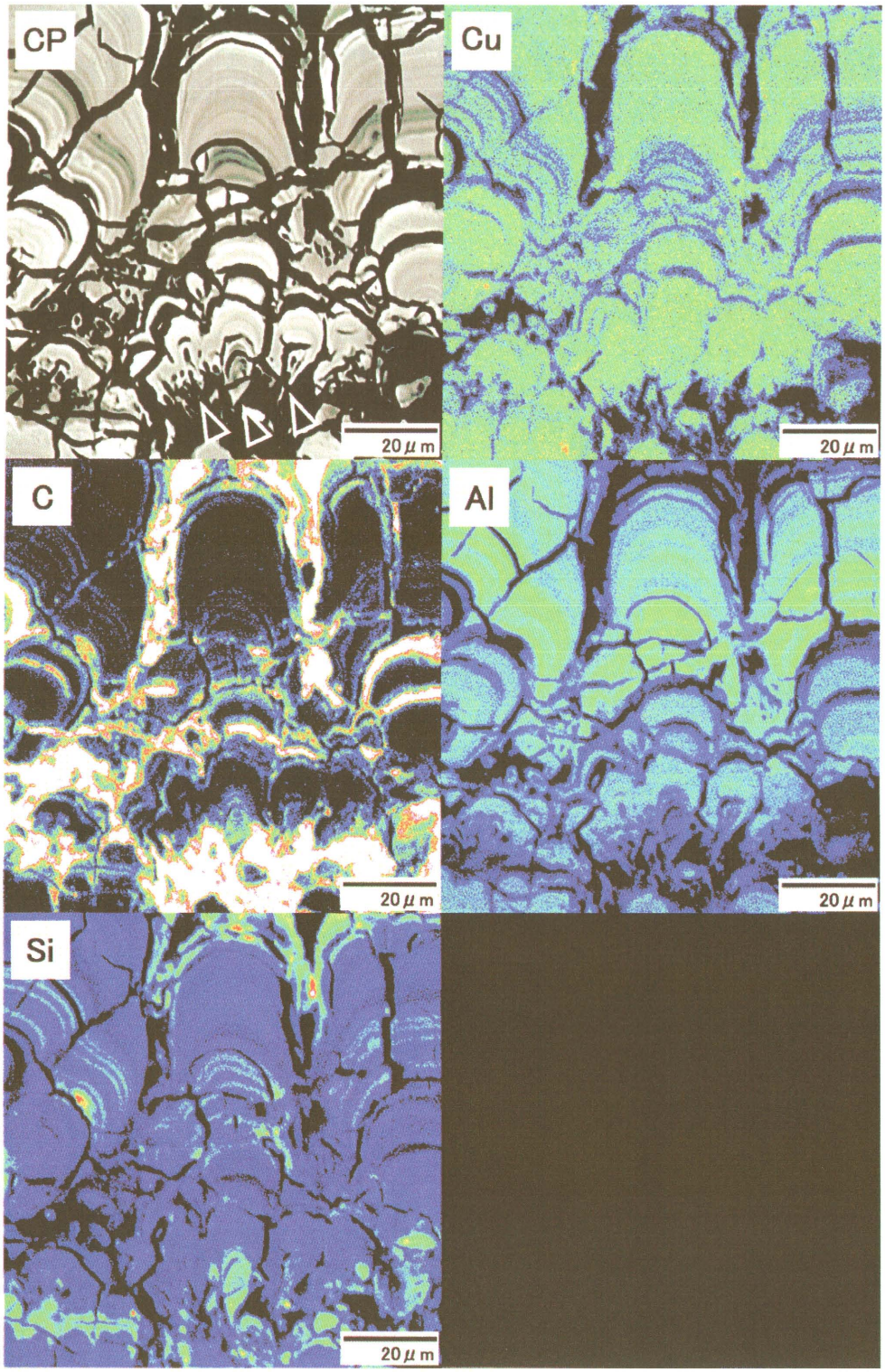


**Fig. 14** EPMA color mapping of green biomats reveals banded elemental distributions. There is tendency that Cu and Al contents are high at the light bands in BEI. Cu and Al are components of woodwardite, while C and Si are high at the dark bands. The sheaths formed at the tips of cyanobacterial filaments (CP, arrows) are also rich in C and Si.

## Blue biomats of Meisei-ko (Point 2)

### Chemical compositions of biomats

Chemical compositions of blue biomats were determined by using EDX-XRF and NCS analyzers. ED-XRF analysis revealed that blue biomats contained large amounts of Cu, Zn, S and Si with traces of Al, Ca, Fe and Pb (Fig. 15). It was apparent that a high Cu peak was remarkable. By comparison, Zn content was more abundant than Cu in the drainage water, while Zn content was lower than Cu in biomats. It was also found that the counts of Cu and Si in blue biomats were higher, while Zn, Al and S were lower than those of green biomats. According to NCS elemental analysis, the result showed that carbon content in the cortical and lower layer of blue biomats was 2.95 wt% and 1.86 wt%, while the nitrogen content in these layers was 2.87 wt% and 1.42 wt%, respectively (Table 1). The contents of nitrogen and carbon in cortical layers were more than those of the lower layers. These were similar to those of the abundant microorganisms in the surface side of blue biomats observed under optical microscope.

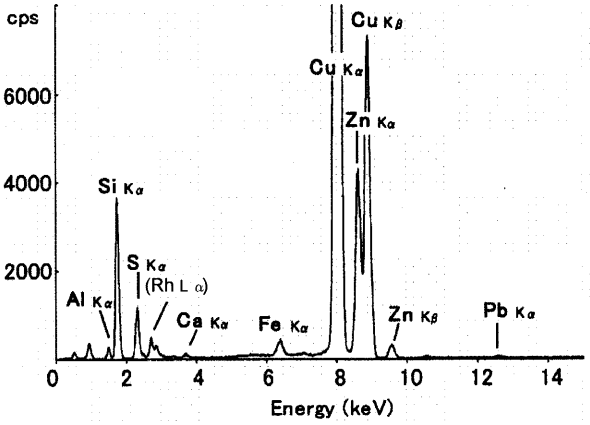


**Fig. 15** ED-XRF analysis of blue biomats. Blue biomats contain large amounts of Cu, Zn, S and Si with traces of Al, Ca, Fe and Pb.

### XRD analyses of blue biomats

XRD pattern showed the broad reflections at 9.3 Å (100), 4.3 Å (41), 2.6 Å (47) and 1.5 Å (37) (Fig. 16) which was similar to Cornwall woodwardite (9.1 (vs), 4.43 (w), 2.58 (m), 1.5 (m): Nickel 1976). Based on the ED-XRF analysis, the findings showed that blue biomats were also composed of Si, Ca, Fe, Zn and Pb. Furthermore, XRD analyses were undertaken to examine the stability of blue biomats at temperatures of 30 to 120 ℃ with interval of 30 ℃ (Fig. 16). The basal spacing of woodwardite in blue biomats decreased progressively up to 7.8 Å at 120 ℃, and its intensity declined gradually. The reflection of 4.43 Å decreased at above 90 ℃. It was apparent that the reflection of 2.60 Å was almost constant.

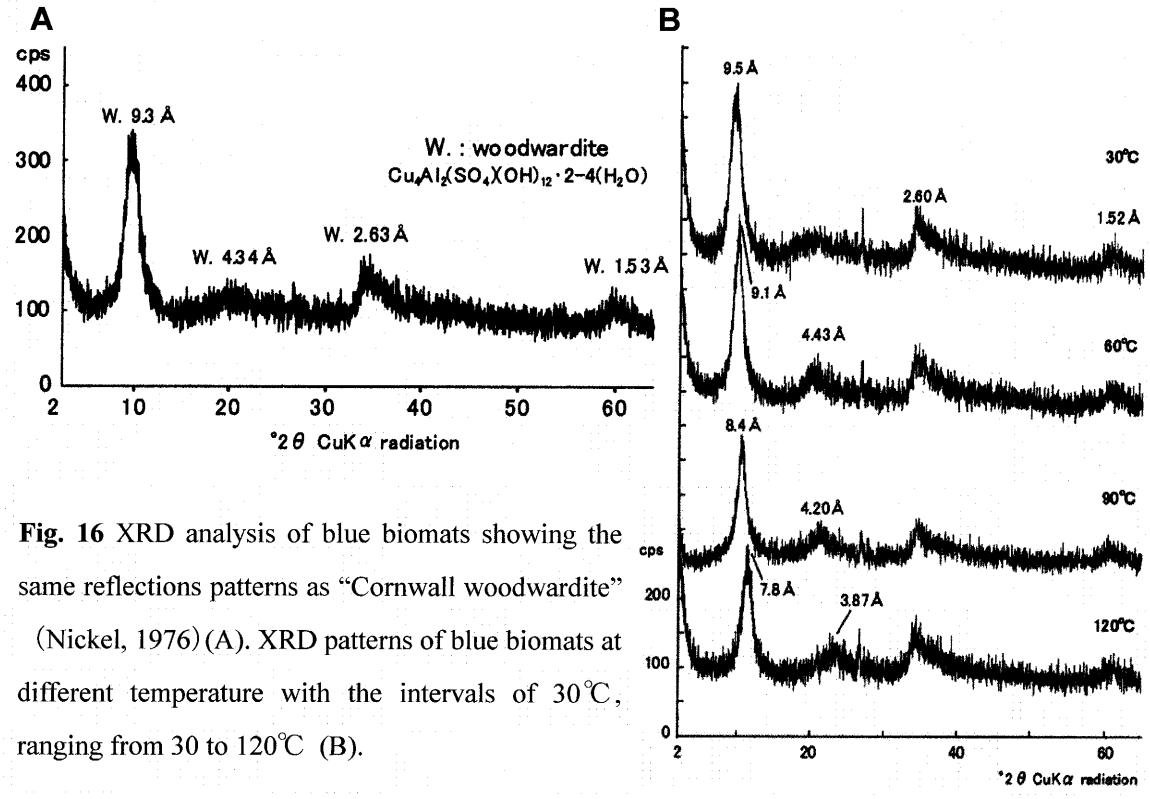


**Fig. 16** XRD analysis of blue biomats showing the same reflections patterns as "Cornwall woodwardite" (Nickel, 1976) (A). XRD patterns of blue biomats at different temperature with the intervals of 30℃, ranging from 30 to 120℃ (B).

## FT-IR spectroscopy of blue biomats

IR spectrum of columnar sheath in blue biomats indicated the presence of organic substances in its grain showing bands at 3700-3100 $cm^{-1}$ (O-H stretch), 2921 $cm^{-1}$ (C-H stretch), 1625 $cm^{-1}$ (C=O stretch), 1247 $cm^{-1}$ (C-H stretch) and 1039 $cm^{-1}$ (Si-O stretch) (Fig. 17). The C-H and C=O bands indicated that the presence of organic substances were derived from microbial cells of blue biomats.

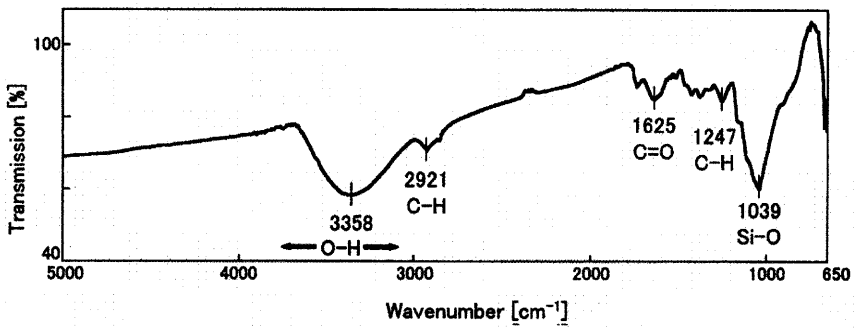


**Fig. 17** FT-IR spectrum of blue biomats indicating the presence of organic substance in the grain, shows the bands at 3700-3100 $cm^{-1}$ (O-H stretch), 2921 $cm^{-1}$ (C-H stretch), 1625 $cm^{-1}$ (C=O stretch), 1247 $cm^{-1}$ (C-H stretch) and 1039 $cm^{-1}$ (Si-O stretch).

**Optical microscopic observations of blue biomats**

Biomats were observed with differential interference and episcopic fluorescence microscope. The columnar, domal and spherical grains which were of translucent to green or sometimes brown in color were observed in the blue biomats (Fig. 18).

Besides that, the columnar to rhombohedral blue grains were also recognized, showing a stromatolite-like micro lamination (Fig. 18A). DAPI-stained samples displayed red and blue fluorescence under the ultraviolet ray that confirmed the

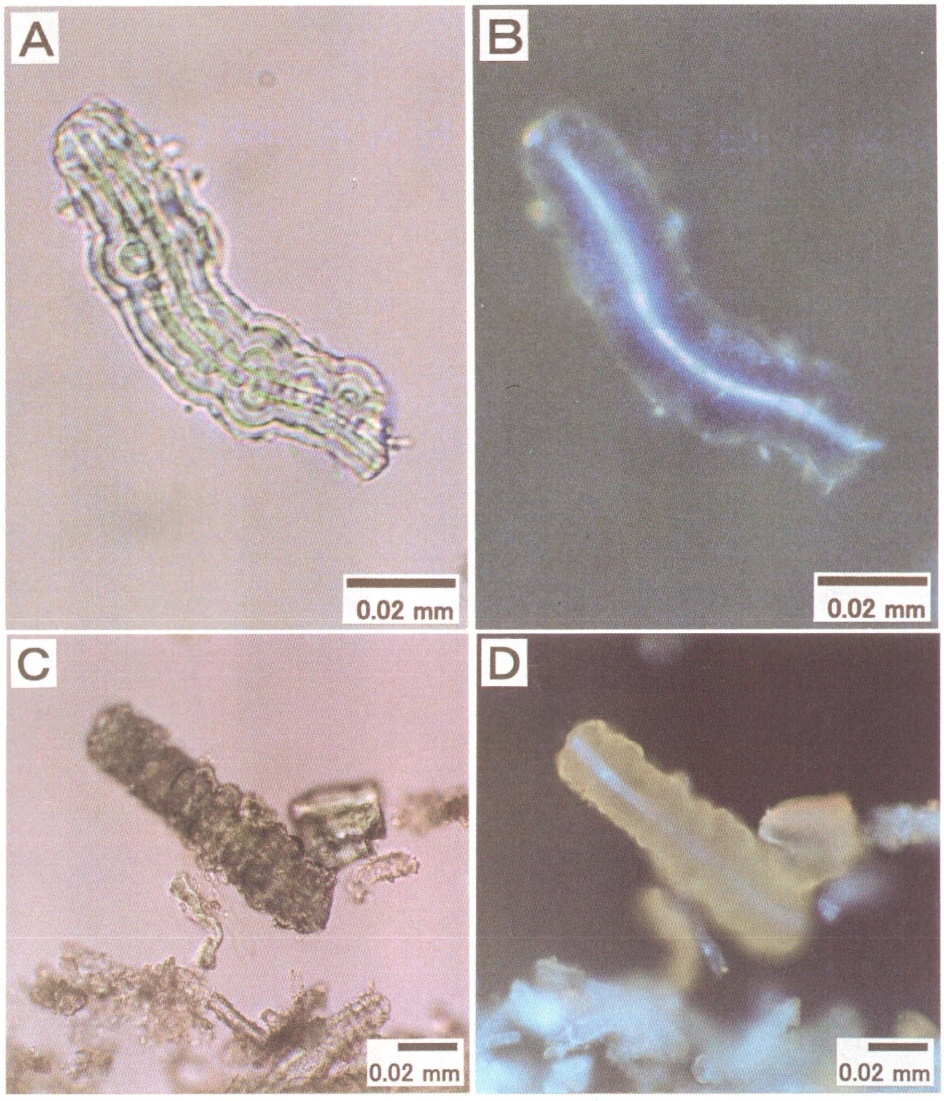


**Fig. 18** Differential interference (A, C) and fluorescence microscopic (B, D) images of blue biomats. Filament is covered with columnar sheath showing lamination and colloform texture (A, C). DAPI-stained samples display red and blue fluorescence under the ultraviolet ray that confirms the presence of chlorophyll and DNA in organism respectively (B, D).

presence of chlorophyll and DNA, respectively (Fig. 18B, D) indicating the presence of living microorganisms. These were adhered with fine granules, and covered with crystalline sheath. In particular, cyanobacteria were among the predominant and characteristic microorganisms in the blue biomats. Most of them were completely encrusted with columnar sheaths (Fig. 18). Sheaths indicated the colloform structure around the cyanobacterial filaments. It was also found that the structure was formed around microorganisms attached on the cyanobacterial filament and sheath. Cyanobacteria were mainly of filamentous typed that formed the non-arborization filament. A cell was 1 to 2 or 5 to 8 μm in diameters, and 2 to 10 μm (generally 3 to 4 μm) in length. The red fluorescence of chlorophyll and blue fluorescence of DNA for non-sheathed filaments were distinct, while sheathed ones were often weak or not detected.

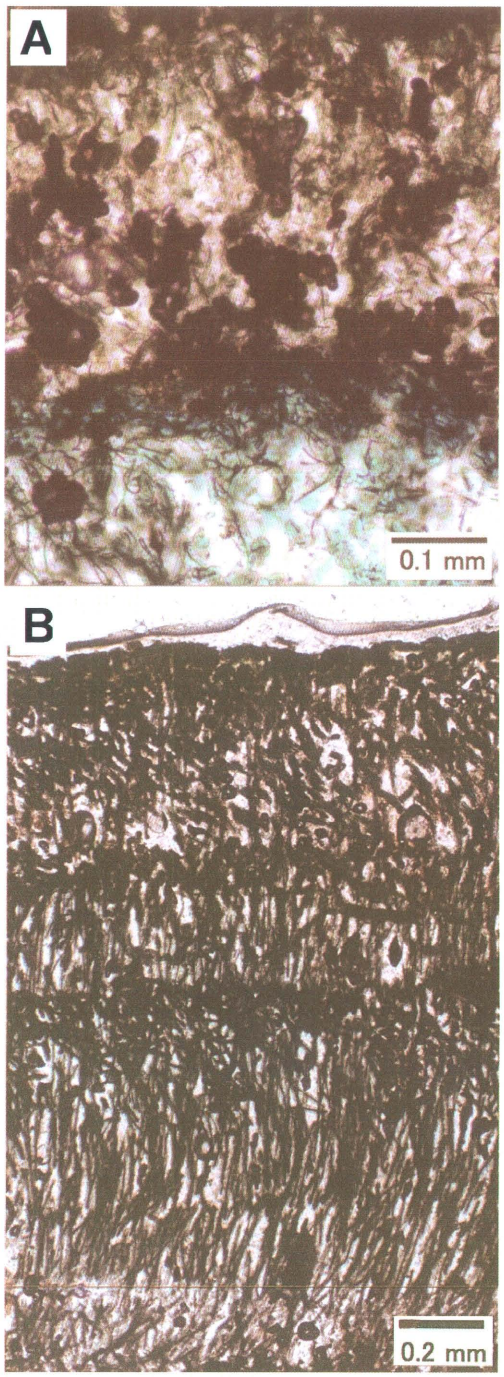


Furthermore, thin sections of blue biomats were observed with polarization-microscope showing the presence of dense and porous layers in biomats where they appeared alternatively (Fig. 19A, B). A set was arranged by these two layers with thickness of 0.3 to 0.4 mm. The set appeared repeatedly resulting in the formation of layered structure where a

**Fig. 19** Polarization-microscopic images of blue biomats showing the dense and porous layers which appear alternatively. The columns are sheathed with cyanobacteria. Cyanobacteria grow towards to the top of biomats. In the dense layer, they grow horizontally.

large number of filamentous microorganisms were found. Based on their morphologies and episcopic fluorescence microscopic observations, they were identified to cyanobacteria. Cyanobacteria grew horizontally in the dense layers, while vertically in porous layers. They could also grow to intertwine (Fig. 19A).

In blue biomats, the columnar sheath formed on cyanobacteria. It was apparent that whole of the cyanobacterial filament was covered with crystalline sheaths (Fig. 20).

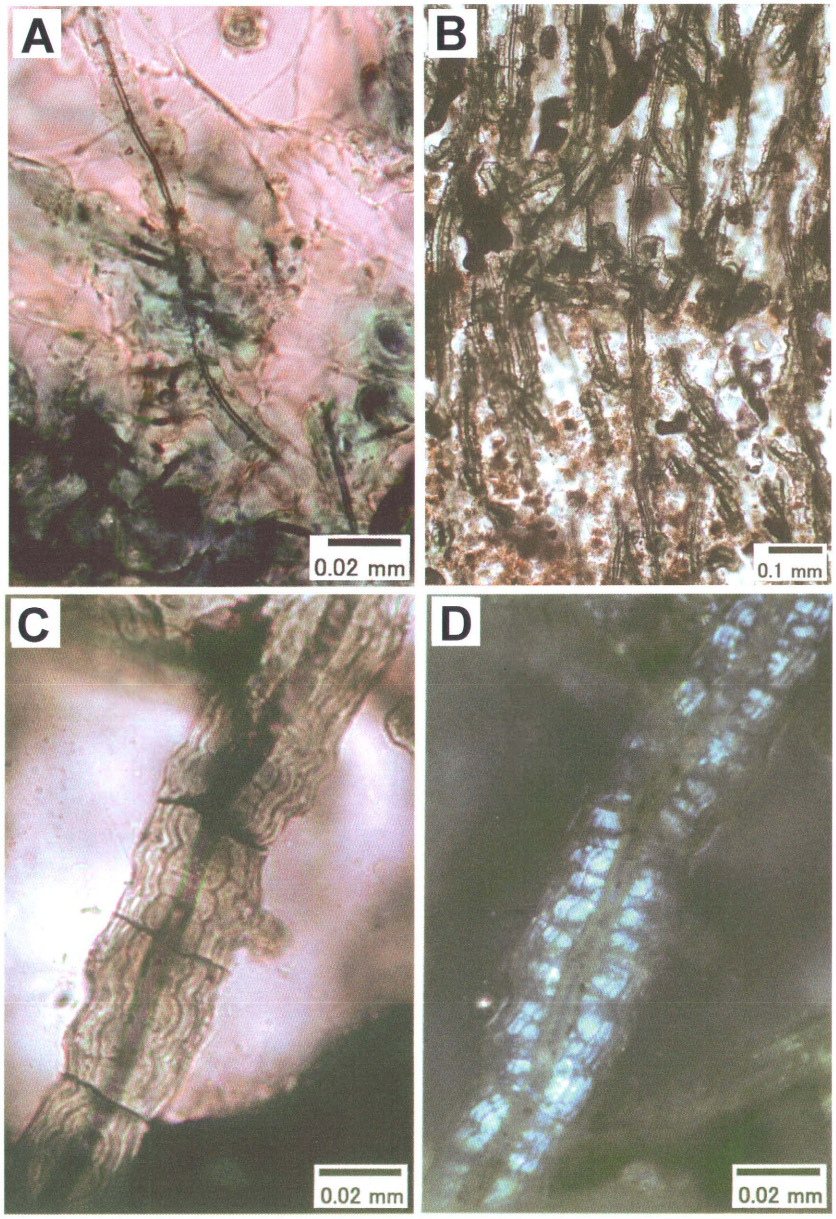


**Fig. 20** Polarization microscopic images of blue biomats in close-up of Fig. 19A (A) and Fig. 19B (B-D). Cyanoacteria are completely covered with sheaths. Colloform texture is developed around the cyanobacterial filaments (C: open polar, D: cross polar).

Moreover, concentric banding was also observed in the sheath. The thickness of the sheath ranged between ~ 0.01 and ~ 0.03 mm. Also, colloform structure was formed on each of the cell consisting of cyanobacterial filaments where microorganisms were also found in the crystalline sheaths (Fig. 20C). XRD analysis identified the presence of minerals (Wodwardite) in biomats which was transparent to pale green in color observed under the microscope. In this case, Pleochroism of minerals was not found, however blue minerals were found (Fig. 19A, 20B). These were dioptase and shattuckite occurring as columnar sheath according to the results of EPMA analysis.

**SEM observations of blue biomats**

In the vertical section, the difference in occurrences of cyanobacteria and grains with dense and porous layer were recognized (Fig. 21 A). As a general tendency, cyanobacteria grew horizontally in the dense layer and vertically in the porous layer. It was observed that there was a variety of microorganisms in the biomats such as cyanobacteria, green algae, spherical microorganisms and organic substances in

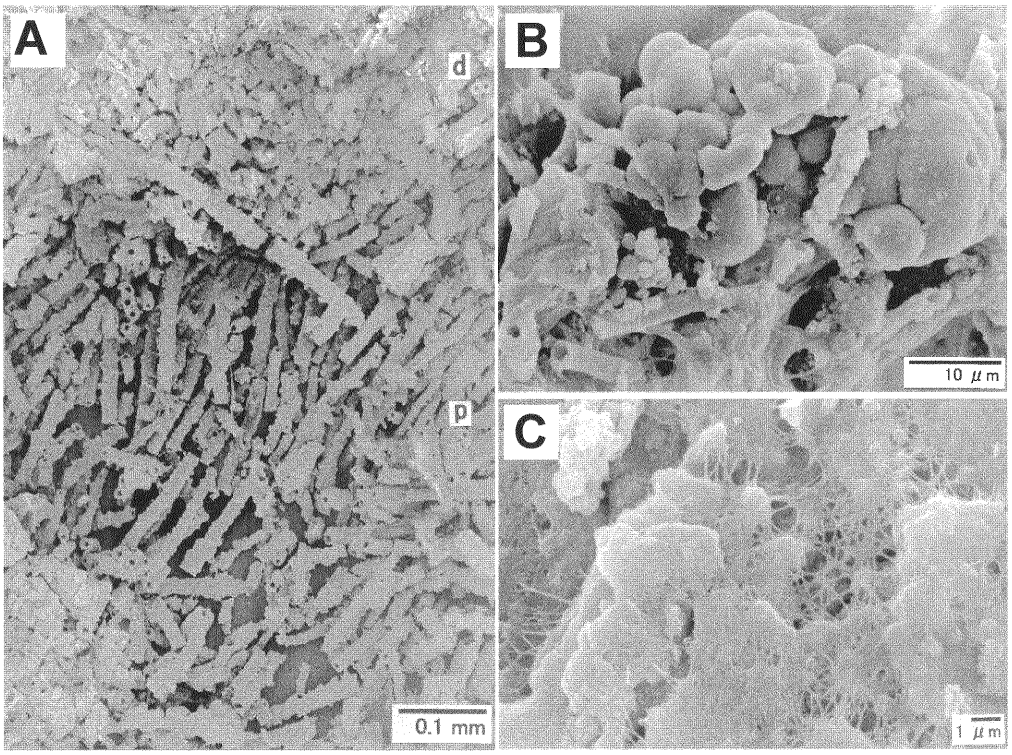


**Fig. 21** Secondery electron images of blue biomat illustrating dense (d) and porous (p) layers (A). Cyanobacteria are covered with columnar sheath. Spherules and sheathed cyanobacteria in aggregation (B) form slime layers (C) in biomats.

association with inorganic matters (Fig. 21B, C). In this case, cyanobacteria were the most predominant than those of other microorganisms and most of particles attached on cyanobacterial cell. Apparently, columnar sheaths formed around cyanobacterial filaments were characteristic where their surface was mostly uneven. As well, it was observed that the cyanobacteria, other microorganisms, organic substance and mineral particles remained together in aggregation associated with sheaths arranging oriented direction (Fig. 22A). The sheaths were gnarled with node having the interval of about 4 μm. These intervals were related to the length of cyanobacterial cells observed with optical microscope. Additionally, EDX analysis showed that sheaths and grains in biomats contained mainly Al, Si, S, Cu and Zn (Fig. 22B). Same as bulk analysis with ED-XRF (Fig. 15), peak of Cu was higher than that of Zn. Occasionally, Si-Cu compounds and the higher Fe-bearing grains were recognized. Moreover, in BEI observation of thin section, the compositional concentric banding was remarkable (Fig. 23). It was also found that a small number of microorganisms existed in the dark circle and groove (arrows in Fig. 23). Apparently, the layer and dome showing stromatolite-like banding were built by aggregation of sheathed cyanobacteria growing in horizontal and vertical direction (Fig. 23).

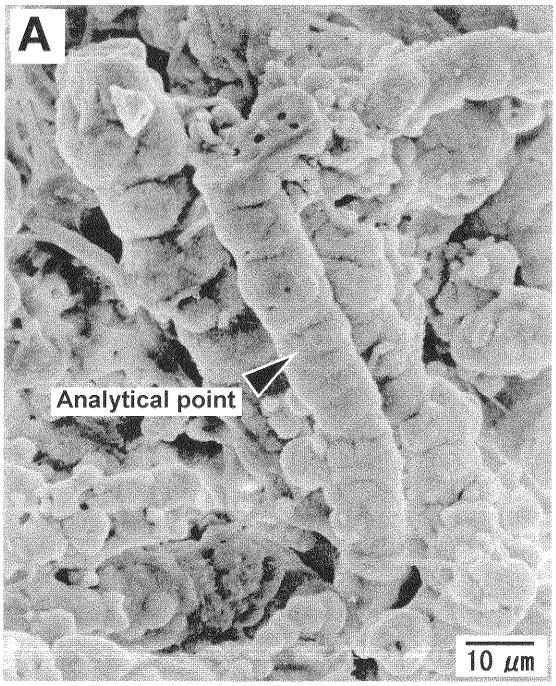


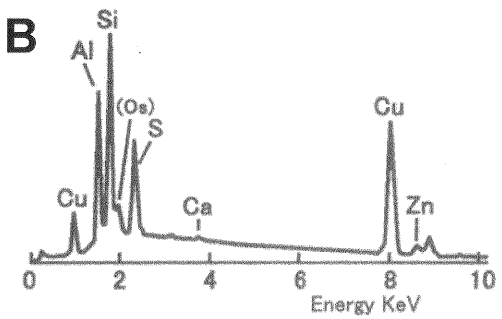


**Fig. 22** Secondery electron images (A) and EDX spectrum (B) of blue biomat illustrating sheathed and non-sheathed cyanobacteria in association with elements. These sheaths are gnarled. Holes at the tips of the columns are traces of cyanobacterial cell. Sheaths consist mainly of Al, Si, S, Cu and Zn with the trace of Ca (B: Os: Os-coating).

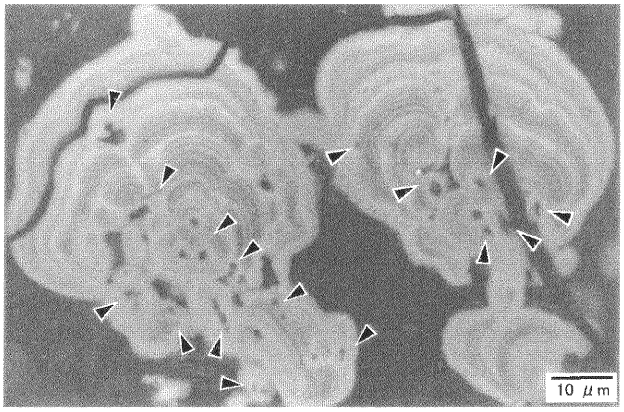


**Fig. 23** Back-scattered electron images of thin sectioned blue biomats showing the domes and stromatolite-like structures that are built by sheathed cyanobacteria growing in horizontal and vertical direction. Arrows show a small number of microorganisms.

**TEM observation of blue biomats**

TEM observations revealed the filamentous cyanobacteria that had thick extracellular sheath (Fig. 24A). It seemed that particles were attached on cyanobacteria and mostly large grains occured on the cells. Generally, fine spherules and flakes were observed (Fig. 24B).

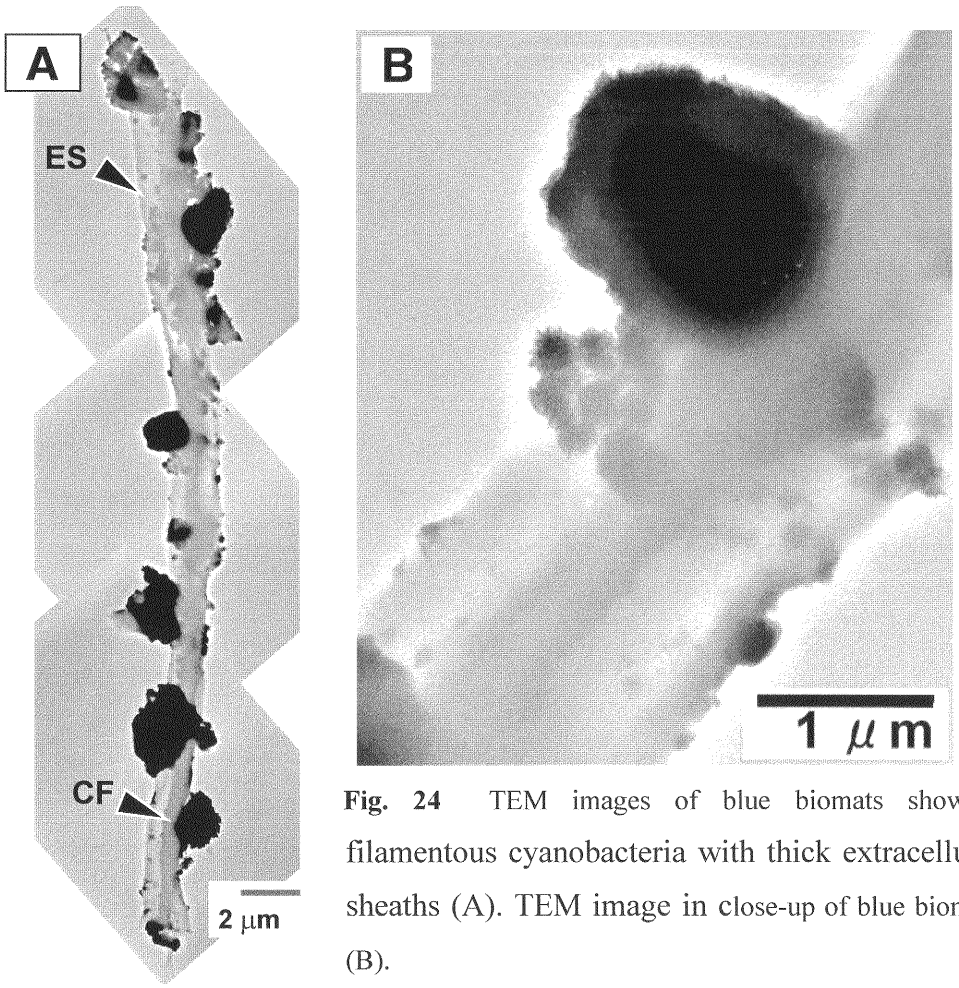


**Fig. 24** TEM images of blue biomats showing filamentous cyanobacteria with thick extracellular sheaths (A). TEM image in close-up of blue biomats (B).

**EPMA analyses of blue biomats**

Whole parts of blue biomats were composed of Al, Si, S, Cu and Zn. EPMA elemental mapping of Al, Si, Cu and Zn revealed complicated elemental distributions. Apparently, there were tendencies that Cu content was high at the light bands in BEI (Fig. 25), suggesting the Cu, Al and S were components of woodwardite. It was also apparent that C and Si were high at the dark bands (Fig. 25). Furthermore, color maps of columnar sheath also showed the high concentrations of C and Si around cyanobacterial filaments (Fig. 25). In general, there was the same elemental distribution of Cu, Al and S, while the distribution of C and Si was also found similar.

Therefore, quantitative analysis results are given in Table 3. The translucent to green parts observed under the optical microscope (woodwardite) contained 51 ~ 59 wt% CuO, 2 ~ 4 wt% ZnO, 7 ~ 14 wt% $Al_2O_3$, 6 ~ 9 wt% $SO_3$, 9 ~ 21 wt% $SiO_2$, and trace amounts of FeO and PbO. As $SiO_2$ is excepted, total weight percents are low, because they contain interlayer and constitution water. It was found that blue biomats was rich in Cu and poor in Al compared with that of green one. The blue biomats showed higher Cu/Al ratio (Table 3) than that of green ones (Table 2). Clearly, Al content was decreased, contrary Cu was increased. The blue parts composed of 45 ~ 57 wt% CuO, 3 ~ 5 wt% ZnO, 0 ~ 2 wt% $Al_2O_3$, 1 ~ 4 wt% $SO_3$, and 32 ~ 36 wt% $SiO_2$. Compositionally, they were identified as dioptase ($CuSiO_2(OH)_2$) and shattuckite ($Cu_5(SiO_3)_4(OH)_2$).

**Table 3** Electron microprobe analyses of blue biomats. Low total wt% is due to adsorptive and crystallin water.

| | woodwardite | | | | | shat. | dioptase | | |
|---|---|---|---|---|---|---|---|---|---|
| FeO | 0.04 | 0.00 | 0.02 | 0.11 | 0.47 | — | — | — | — |
| CuO | 58.61 | 55.57 | 55.02 | 51.08 | 56.51 | 56.75 | 49.31 | 46.12 | 45.72 |
| ZnO | 3.76 | 4.00 | 3.66 | 2.35 | 4.14 | 3.39 | 4.14 | 4.38 | 4.22 |
| PbO | 0.36 | 0.27 | 0.14 | 0.49 | 0.00 | — | — | — | — |
| Al2O3 | 7.53 | 8.67 | 8.96 | 7.64 | 13.94 | 0.21 | 0.26 | 1.58 | 0.19 |
| SO3 | 6.05 | 5.94 | 7.10 | 8.21 | 9.10 | — | — | — | — |
| SiO2 | 17.61 | 19.31 | 21.14 | 8.92 | 12.19 | 34.09 | 32.79 | 35.38 | 35.75 |
| Total | 93.96 | 93.76 | 96.03 | 78.78 | 96.35 | 94.43 | 86.50 | 87.45 | 85.88 |
| | Cations per 10 oxygens calculated except for silica | | | | | Cations per X oxygens X=13 for shat. and 3 for dioptase | | | |
| Fe | 0.005 | 0.000 | 0.002 | 0.012 | 0.043 | — | — | — | — |
| Cu | 5.974 | 5.696 | 5.460 | 5.321 | 4.677 | 4.892 | 1.051 | 0.936 | 0.946 |
| Zn | 0.374 | 0.401 | 0.355 | 0.239 | 0.335 | 0.286 | 0.086 | 0.087 | 0.085 |
| Pb | 0.013 | 0.010 | 0.005 | 0.018 | 0.000 | — | — | — | — |
| Σ | 6.366 | 6.107 | 5.822 | 5.590 | 5.055 | 5.178 | 1.137 | 1.023 | 1.032 |
| Al | 1.197 | 1.387 | 1.387 | 1.242 | 1.800 | 0.028 | 0.009 | 0.050 | 0.006 |
| S | 0.613 | 0.604 | 0.700 | 0.849 | 0.748 | — | — | — | — |
| Si | — | — | — | — | — | 3.890 | 0.925 | 0.951 | 0.980 |
| Total | 8.176 | 8.098 | 7.909 | 7.681 | 7.603 | 9.096 | 2.071 | 2.024 | 2.017 |

shat.: shattuckite Total Fe as FeO

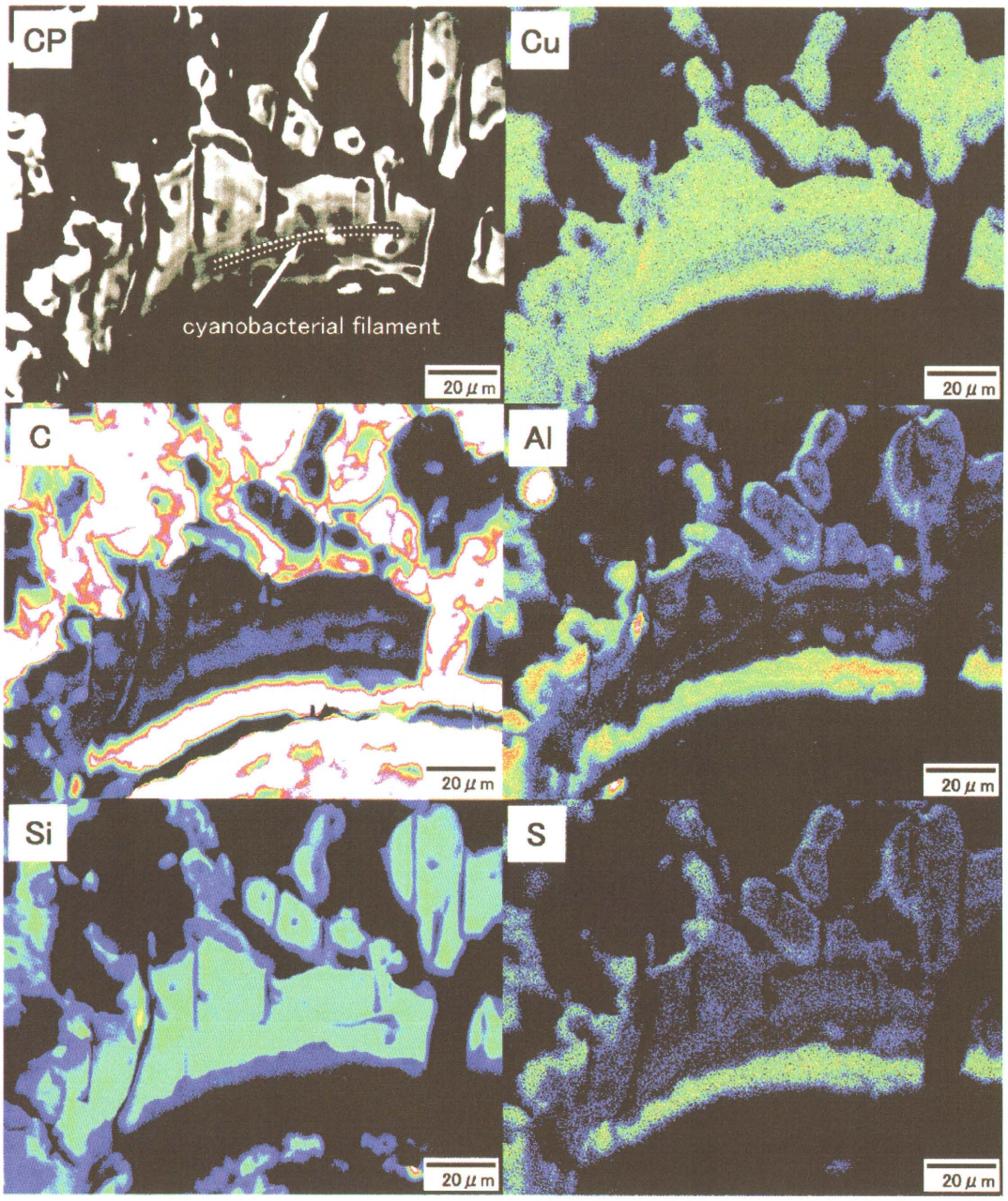


**Fig. 25** EPMA color mapping of blue biomats reveals banded elemental distributions showing high Cu content at the light bands in BEI. Whereas, the Cu, Al and S are components of woodwardite showing high C and Si at the dark bands and around cyanobacterial filaments. Both Si and Cu are distributed at the same area.

## DISCUSSIONS

In the present work, the vivid green and blue biomats formed in the Cu and Zn-drainage water at Dogamaru mine, Shimane Prefecture, Japan, consisted of a variety of microorganisms particularly cyanobacteria in association with copper minerals. Cyanobacterial cell was 1 - 4 μm in diameter, and 2 - 10 μm (average 3 - 4 μm) in length. Significantly, filamentous cells have no arborized form nor contracted joint. The cyanobacteria has such characterlistics as *Oscillatoria* spp. and *Phormidium* spp. (Holt et al. 1994; Kojima et al. 1995). Particularly, *Phormidium* was of the superior species in the heavy metal contaminated river (Kojima et. al 1995). In addition, the stromatolite-like banded structures were also shown in these biomats. Copper-biomineralization and stromatolite-like banded structures were discussed as follows. Large amounts of heavy metals such as copper, zinc, manganese and iron were found in the metal mine drainage system. They usually brought some problems to be contaminants to soil and water environments. In this study at Dogamaru mine also contained large amounts of Cu and Zn ranging from 2.6 to 2.7 ppm and 28.1 to 29.5 ppm, respectively (Table 1). These values were approximately 380 and 1000 times higher than that those in the general river of the world, which had the Cu and Zn concentrations of 10 μg/l and 30 μg/l respectively (Martine and Meybeck 1979). In addition, numerous microorganisms existed in the biomats even in such high heavy metal contaminating surrounding environments, and fixed large amounts of Cu and Zn as minerals.

### Cu-minerals in biomats at Dogamaru mine

Green and blue biomats were found in comparatively wide range at Dogamaru mine drainage system (Watanabe and Tazaki 1998a, 1998b) (Fig. 2). The biomats contained copper minerals, mainly woodwardite with the small amounts of dioptase and shattuckite (Watanbe and Tazaki 1999, 2000). Woodwardite has been described for occurrence and mineralogy (Nickel 1976; Takada and Matsuuchi 1981; Raade 1985; Livingstone 1990; Witzke 1993) even though it was rare in occurrence. Generally speaking, woodwardite was a secondary mineral in oxidized zone of ore deposits. This mineral occured as crusts on the mining waste rocks, in the crack and the void (Takada

and Matsuuchi 1981; Witzke 1993, 1999). Woodwardite was originally reported from Cornwall. The Formula was given as probably $Cu_4Al_2(SO_4)(OH)_{12} \cdot 2\text{-}4H_2O$. XRD data alleged woodwardite from Caernarvonsire, Wales, was given in the JCPDS file under the No. 39-0726. As well, Nickel (1976) pointed out discrepancies in XRD data between Caernarvonsire specimen and Cornwall specimen (Table 4) wherein particularly notable was the large basal spacing of 10.9 Å versus the 9.1 Å basal spacing of Cornish samples. On the expectation that Caernarvonshire specimen represented a hydrated equivalent of the Cornish woodwardite in which Nickel (1976) conducted XRD analyses for both samples at temperature intervals of 30 ℃. The results showed that the basal spacing of the Cornish sample decreased progressively to 8.1 Å at 120 ℃, whereas the basal spacing of the Caernarvonsire material disappeared all lines at 90 ℃. He explained that Caernarvonsire specimen was not simply a hydrated version of the Cornish woodwardite. In addition, the Cu : Al atomic ratio in the Cornish sample was found to vary between 1.73 and 2.03. On the other hand, the Caernarvonsire material gave Cu : Al ratios between 0.62 and 0.82. Thus, Nickel (1976) concluded that they did not represent the same mineral, because of XRD data, degree of structural stability under increasing temperature and Cu : Al ratios were incompatible.

**Table 4** XRD data for woodwardite in JCPDS file and Nickel (1976).

| JCPDS file | | Nickel (1976) | |
|---|---|---|---|
| d (Å) | I | d (Å) | I |
| 10.9 | 100 | 9.1 | vs |
| 5.46 | 60 | 4.43 | w |
| 3.66 | 50 | - | - |
| 2.613 | 40 | 2.58 | m |
| 2.454 | 20 B | - | - |
| 1.535 | 5 B | 1.5 | m |

Besides that, Witzke (1999) described the new mineral hydrowoodwardite ($[Cu_{1-x}Al_x(OH)_2][(SO_4)_x/2(H_2O)_n]$ with $x < 0.67$ and $n > 3x/2$) at Saxony, Germany. Hydrowoodwardite was higher hydrated analogue of woodwardite. Witzke (1999) explained that hydrowoodwardite was identical with Caernarvonshire mineral described by Nickel (1976), however Nickel (1976) explained that Caernarvonsire specimen was not simply a hydrated version. In addition, Witzke (1999) reported that hydrowoodwardite and woodwardite were trigonal. Woodwardite and hydrowoodwardite had a hybrid layer structure of brucite-like ($M^{2+}$, $M^{3+}$)-layers and anion-water-interlayers. Woodwardite and hydrowoodwardite were associated to hydrotalcite group minerals (hydrotalcite: $Mg_6Al_2(OH)_{16}CO_3^{2-} \cdot 4H_2O$). Minerals of

hydrotalcite group exhibited trigonal symmetry and a cell or subcell with a'=3.0 Å and c'=7.5 ~ 11.3 Å (according to the interlayer structures) (Witzkl 1999). This group was called layered double hydroxides (LDHs). Recently, LDHs was attended in the view point of earth chemistry, because LDHs intercalated the biomolecules in living system such as amino acids, polypeptides, sugars and nucleic acids (Narita 2001). Likewise, basal spacing of LDHs was changed by kinds of intercalated biomolecules. Chemical formula of LDHs was represented to [M1-x2+Mx3+($OH_2$)][Ax/mn- · y$H_2O$] ($M_x^{2+}$: Ca, Mg, Ni, Zn, etc.; $M_x^{3+}$: Al, Fe, Cr). Chemical formula of woodwardite was $Cu_4Al_2(SO_4)(OH)_{12}$ · 2-4($H_2O$). Replacement of $Cu^{2+}$ by $Al^{3+}$ ($M^{2+}$ by $M^{3+}$), coupled with $SO_4^{2-}$ for charge balance, and replacement of $Cu^{2+}$ by $Zn^{2+}$ (or other divalent cations) were reported for hydrowoodwardite by Witzke (1999). The formula $Cu_{5\text{-}5.5}Al_{2.5\text{-}3}[(OH)_{16}/(SO_4)_{1.2\text{-}1.5}]$ · n($H_2O$) as Cu analogue of glaucocerinite ($(Zn,Cu)_5Al_3(SO_4)1.5(OH)_{16}$ · 9($H_2O$)) was also reported by Witzke (1993). Livingstone (1990) suggested $Cu_6Al_2(SO_4)(OH)_{16}$ · 7($H_2O$) (52.3 wt% CuO, 11.2 wt% $Al_2O_3$, 7.0 wt% $SO_4$, 29.5 wt% $H_2O$) as Cu-Al analogue of hydrohonessite ($Ni_6Fe_2(SO_4)(OH)_{16}$ · 7($H_2O$) ), when allophane was coexisted with woodwardite.

Furthermore, XRD patterns of the green biomats of Point 1 at Dogamaru mine were similar to Caernarvonsire woodwardite (Fig. 4A, Table 4). Chemical composition also matched with general formula of woodwardite ($Cu_4Al_2(SO_4)(OH)_{12}$ · 2-4$H_2O$) as exception for data showing low (Cu+Zn+Pb) / Al ratios (Table 2). In Point 2 samples, XRD patterns of the biomats were similar to Cornwall woodwardite (Fig. 16A, Table 4). However, they demonstrated high (Cu, Zn, Pb) / Al ratios (Table 3). These ratios were compositionally closer to Cu-Al analogue of hydrohonessite ($Ni_6Fe_2(SO_4)(OH)_{16}$ · 7($H_2O$)) suggested by Livingstone (1990). Woodwardite might show the Cu-rich and Al-poor compositions in Point 2. Woodwardite commonly coexisted with Cu-bearing allophane and amorphous silica (Nickel 1976; Livingstone 1990; Witzke 1993, 1999). At Dogamaru mine, Si was always detected whereas other Cu minerals (such as dioptase and shattuckite) were also identified. The biomats of point 2 were mixture of these amorphous materials and Cu minerals.

Biomineralization of copper have been reported (Little et al. 1997). McNeil et al. (1991) observed morphology of copper sulfide deposited on the bacterial cell in

biofilms with corrosion experiment of copper films. Tazaki et al. (1992) also reported the accumulation of Al-Fe-Cu-Zn phosphate by bacteria in the experiment using activated sludge. In the nature, Kishigami et al. (1999) described native copper and cuprite in biomats from Ogoya mine, Ishikawa Prefecture. However, there were no reports on relationship between woodwardite and microorganisms.

## Copper-tolerance and accumulation mechanisms by microorganisms

Transition metal ions, especially not only iron but also copper and zinc, were essential for life. For instance, copper and zinc constituted blue copper proteins for electronic transported reaction. Copper-zinc superoxides behave in a decomposition of superoxide ion, DNA and RNA polymerase for metabolism of nucleic acid. Since they became toxic at higher concentrations, organisms have developed resistance mechanisms to toxic metals to make innocuous. Organisms responded to heavy metal stress by using different defense systems, such as exclusion, compartmentalization, making complex and the synthesis of binding proteins (Lippard and Berg 1994; Mejare and Bulow 2001). Numerous studies have been conducted on accumulation and tolerance for bacteria and algae in the cultivation experiment (Ledin 2000). About copper and zinc, there were many reports for various microorganisms such as Cyanophyceae (*Phormidium* spp., *Chamaesiphon subglobosus Lemm*), yeast (*Candida* sp, *Kluyveromyces marxianus*, *Saccaromyces cerevisiae*), *Escherichia coli*, *Ferrobacillus ferrooxidans*, *Thiobacillus thiooxidans*, *T. ferrooxidans*, *Pseudomonas aeruginosa*, *P. syringae*, *Bacillus megaterium*, *B. subtilis*, *B. polymyxa*, *B. cereus*, *Desulfovibrio desulfurican* etc. (Booth and Mercer 1963; Temple and Le Roux 1964; Kikuchi 1965; Yamamoto et al. 1985; Takamura et al. 1989; Panchanadikar and Das 1993; Coosey 1994; Sze et al. 1996; Das et al. 1997; Morsi Abd-El-Monem et al. 1998; Wang et al. 1998; Donmez and Aksu 1999; Kotba et al. 1999; Chen et al. 2000; Gadd 2000; Mejare and Bulow 2001). Microorganisms possessed metallochaperone that guided and protected transition metal ions within the cell, delivering them safely to the appropriate protein receptors, in order to avoid excess levels that were toxic for living body (Lippard 1999). Alcaligenes eutrophus precipitated heavy metals in periplasm (Omori et al. 2000). *Pseudomonas syringae* had copper binding protein concern with

blue $Cu^{2+}$ ion delivery in the periplasm and outer membrane (Coosey 1994; Silver 1997). Storage of excess copper in the periplasmic space between the outer and inner cell membranes protects the cell from toxic copper (Coosey 1994; Silver 1997; Omori et al. 2000). Yeast having copper tolerance fixed copper ion inside the cell wall as sulfide, and protected the cell from toxic copper (Ashida et al. 1963; Kikuchi 1965).

The various peptides consisting of metal-binding amino acid (mainly histidines and cysteines) have been studied for heavy metal binding capacity, tolerance or accumulation by microorganisms and plants (Kotrba et al. 1999; Gadd 2000; Mejare and Bulow 2001). Naturally occurring Cd-binding proteins and peptides, such as metallothioneins or phytochelatins, were very rich in cysteines. In addition, histidines were well known to have a high affinity for transition metal ions such as $Cu^{2+}$, $Zn^{2+}$, $Co^{2+}$ and $Ni^{2+}$ (Mejare and Bulow 2001). Cyanobacteria and algae produced metal-binding proteins which internally sequestered and detoxified high concentrations of metals within the cell (Humble et al. 1997). Humble et al. (1997) also reported binding of copper and zinc to cyanobacterial microcystins. Microcystins were family of hepatotoxic heptapeptides which had been detected in wide range of cyanobacteria.

In heavy metal rich environment, tolerant species grew and fixed dissolved heavy metals from polluted water by biomineralization (Mann et al. 1987; Ferris et al. 1989; Tazaki 1997). Further, biofilms, surface of microorganisms and extracellular polysaccharides (EPS) served nucleation and deposition sites for ions and particles in solution (Renaut et al. 1998; Konhauser and Urrutia 1999). The electron microscopic observations and experiments revealed that Mn, Fe, Cu, Zn and Ca bearing minerals formed by metabolism were fixed with EPS of various bacteria and cyanobacteria (Tashiro and Tazaki 1999; Banfield et al. 2000; Chen et al. 2000; Yasuda et al. 2000; Ueshima and Tazaki 2001).

In case of Dogamaru mine, copper minerals were always found around microorganisms. DAPI stained samples showed the blue fluorescence of DNA and red fluorescence of chlorophyll (Fig. 6, 18) indicating that microorganisms formed copper minerals while they were living. As well, C-H-N and C-H bonding were detected with FT-IR analyses of grains (Fig. 5, 17). These results strongly confirmed a relationship between mineralization and EPS. It was also seen that cyanobacteria species commonly

had a fibrous extracellular sheath (Watanabe et al. 1994). EPMA color mappings also revealed that crystalline sheath forming around cyanobacteria was rich in carbon (Fig. 14, 25). TEM observations also supported the domination of filamentous cyanobacteria that had thick extracellular sheath (Fig. 11, 24). In addition, fine particles of woodwardite were also recognized on the cellular surface and extracellular sheath of cyanobacteria (Fig. 12). These results indicated the biomineralization of copper minerals by microbial cell and extracellular sheath. Microorganisms recognized in biomats at Dogamaru mine also formed copper minerals around the cell wherein they might contribute to alleviate copper toxicity.

Furthermore, it was seen that Cu content in the biomats was more than that of Zn (Fig. 3, 15), which was inversely proportional to drainage water showing that Zn content was more than Cu (Table 1). It was suggested that biomass had higher affinity for Cu than that of Zn (Sanchez et al. 1999). Complexation of amino acids with metal ions showed that, in general, $Cu^{2+}$ ion were more strongly complexed than $Zn^{2+}$ ions (Humble et al. 1997; Kotrba et al. 1999).

## Stromatolite-like banded structure in biomats at Dogamaru mine

In green and blue biomats, stromatolite-like banded structure were remarkable. Based on the microscopic observations, they consisted of banded structures in mm-order and μm sized lamina. Stromatolites were organosedimentary structures produced by trapping, binding and/or precipitation as a result of the growth and metabolic activity of microorganisms principally cyanophytes. They showed the typical banded structures (Walter 1976). Recently, stromatolite and biomats showing a fine banded structure in the hot springs and mining areas have also been reported. Although calcareous and siliceous stromatolites were well known, yet there were also iron and/or manganese stromatolites (Walter et al. 1976; Renaut and Jones 1998; Leblanc et al. 1996; Akahane and Yasuda 1997; Akai and Akai 1997; Renaut et al. 1998; Kanno and Fujii 2000; Tazaki 2000; Shikaura and Tazaki 2001). It paid attention to these recent stromatolites as the clue for the formation mechanisms of ancient stromatolite and sedimentary ore deposit.

In general, stromatolite banded formation and its periodicity were discussed by

environmental conditions (seasonal and daily changes, tide, physical and chemical changes of solution, eruption period of the geyser) that were organic rather than inorganic (Monty 1976; Walter 1976; Lowe 1994; Kano and Fujii 2000; Pope et al. 2000). Besides that, based on species and growth patterns of microorganisms, various formation patterns and morphologies of stromatolite were described (Monty 1976; Freytet and Verrecchia 1998; Seong-Joo et al. 2000). Furthermore, Walter et al. (1976) reported that each cyanobacteria covered with silica form each of the bands in the siliceous stromatolite at Yellowstone National Park. This evidence showed that stromatolite bands were formed not only by inorganic conditions but also by microorganic activities.

**Banded structure formation in mm-order**

In the biomats of Dogamaru mine, the banded structures in mm-order were distinguished with (1) differences of growth direction of the microorganisms, (2) distribution density of the microorganism and the minerals, and/or (3) crystallinity of layers. Such banded structures were reported by Monty (1976). Bands formation occurred with the various factors such as growth direction of the microorganisms, seasonal activities of microorganisms and deposition rate of the crystal. Kano and Fujii (2000) observed the tufa in every season. They reported that tufa contained numerous cyanobacteria growing towards the top. The distribution densities of calcite crystals encrusted filamentous cyanobacteria were different at summer and winter. Kano and Fujii (2000) also explained that bands formed by seasonal variation in abiotic calcite precipitation rate (large in summer and small in winter), related to the water temperature, $Ca^{2+}$ content and flow strength (Kano and Fujii 2000). As well, Seong-joo et al. (2000) described for millimeter-scale lamination with differences of cyanobacterial species and/or growth direction of filamentous cyanobacteria.

At Dogamaru mine, the green biomats at Point 1 were built in the alternation of low-crystalline to amorphous and crystalline layers (Fig. 7A, B). The low-crystalline to amorphous layer corresponded to organic-rich porous layer in Fig. 8 and 14. Grain size was small in the low-crystalline to amorphous layer indicating that low-crystalline to amorphous layer formation occurred resulting from the amounts of the cyanobacteria

and organic substance increased among blooming and fixation of ions in the waste water occurred rapidly due to the biomineralization, while crystalline layer formation occurred steeply in accordance with the growth of cyanobacteria. Firstly, low-crystalline to amorphous layer formed on surface of rock or previous biomats. Subsequently, filamentous microorganisms grew horizontally. Meanwhile, filaments erected and formed crystalline sheaths around the cell. Eventually, micro lamination developed on the sheaths. Finally, crystalline domal to columnar structures formed. The horizontal arrangement of domal to columnar structures changed into a crystalline layer. Further, the blue biomats at Point 2 were established in the alternation of porous and dense layers (Fig. 19). The growth direction of cyanobacteria was vertical in porous layer and horizontal in dense layer.

Therefore, the banded structures formed by the differences such as cyanobacteria growth direction, distribution, mineral formation, and the crystallinity. It was suggested that banded structures formation occurred by differences in priority species, growth direction and biomineralization rate of microorganisms.

**Micro lamina formation**

There were two micro lamina formations by cyanobacteria as follows:

*(1) Horizontal growth*

Micro lamina formations were in correlation with the width and growth of cyanobacterial cell. As for stromatolite formation associated with cell size, Walter et al. (1976) reported that the algal and bacterial filaments were usually arranged parallel to the lamination, and the thinnest laminae were composed of single algae or bacterial filaments encrusted with silica, in the hot springs of Yellowstone National Park. According to the microscopic observations of biomats at Dogamaru mine, cyanobacterial filaments were arranged parallel to the lamination and thinnest laminae were composed of single cyanobacterial filaments, similar to being reported by Walter et al. (1976) (Fig. 7D). Cyanobacteria stuck around the constructions and growth horizontally (Fig. 9A, 26A) and promoted lamina formation by biomineralization and fixation of grains with cell and/or extracellular sheaths. The compositional lamination was also shown (Fig. 25). The crystalline sheaths showed the compositional concentric

micro laminae consisting of cyanobacterial filamens, carbon-rich layer associated with extracellular sheaths, and mineral layers (Fig. 26B). Finally, these sheaths achieved in aggregates over which micro laminae developed (Fig. 23).

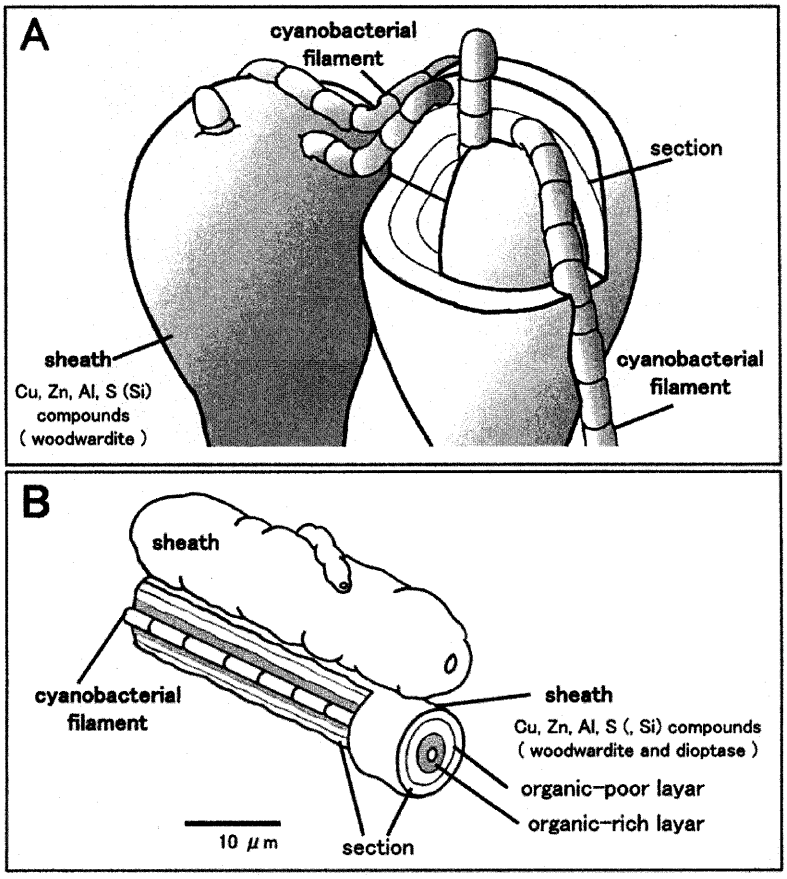


**Fig. 26** Schematic formation of micro lamina regulated by cyanobacterial cell horizontally growing. Cyanobacterial filaments are arranged parallel to lamination and thinnest lamina which are composed of single cyanobacterial filament (A). Compositional lamination showed in (B). Crystalline sheaths indicate compositional concentric micro laminae forming by cyanobacterial filaments with, carbon-rich layer which are associated with extracellular sheath and mineral layers.

*(2) Vertical growth*

Micro lamina was in association with the length of each cell resulting in cyanobacterial filaments. In the biomats of Dogamaru mine numerous cyanobacteria grew towards to surface of biomats, and crystalline sheaths showing micro laminae formation occurred around cyanobacterial cells. Lamina developed upward contemporary with growth of cyanobacteria. In green biomats at Point 1, span of lamina was corresponding to the length of the cell resulting in cyanobacterial filaments (Fig. 10, 27A). In addition, in blue biomats at Point 2, colloform structure was shown in the

sheath (Fig. 18, 20C). Colloform structure formation occurred on each cell resulting in filaments (Fig. 27B). Micro lamination was constructed by arrangement of these sheaths (Fig. 27). This lamina which cyanobacterial cellular size was reflected is a minimum unit of stromatolite-like bands. Freytet and Verrecchia (1998) reported lamina formation resulting in crystallization and diagenesis around the filaments growing vertically. In this study, it was clarified that lamina formation occurred resulting from the biomineralization and width of lamina in correlation with the size of each cyanobacterial cell. This is the first time to show the minimum unit of stromatolite-like banded structure by direct electron microscopic observations.

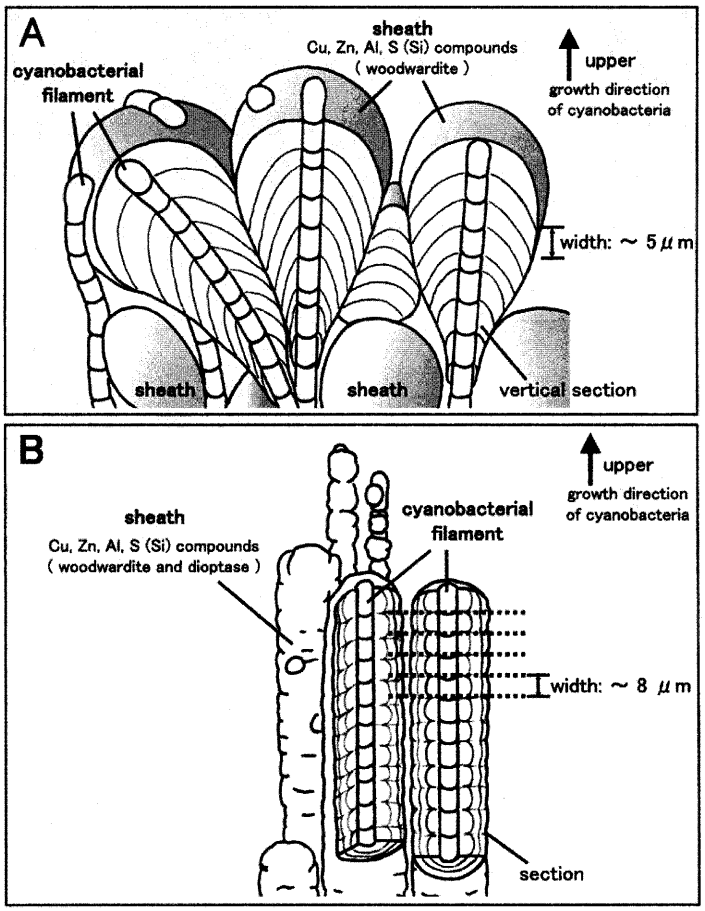


**Fig. 27** Schematic formation of banded textures regulated by cyanobacterial cell vertically growing. In green biomats from Point 1, span of lamina is corresponding to the length of the cell forming cyanobacterial filament (A). In blue biomats from Point 2, colloform structure is shown in the sheath. Colloform structure is formed on each cell forming filament (B). Micro lamination is constructed by arrangement of these sheaths. This lamina which cyanobacterial cellular size was reflected is minimum unit of stromatolite-like banding.

# CONCLUSIONS

Formation of vivid green and blue biomats in the drainage (herein its water contained the large amounts of copper and zinc ions) enclosed to the pits of Dogamaru mine, Shimane Prefecture, Japan resulted in the accumulation of high concentrations of Cu and Zn. The biomats wherein stromatolite-like banded structures formed consisted of various microorganisms and some copper minerals. Microscopic observations of the biomats clearly revealed a close relationship between the filamentous cyanobacteria and stromatolite-like structures formation.

## Biomineralization of Cu ion by microorganisms

Some copper minerals were identified in biomats with XRD and EPMA analyses. Copper minerals were mainly woodwardite with minor amounts of dioptase and shattuckite. At Dogamaru mine, formation of copper minerals occurred around microorganisms among which cyanobacteria were of the most predominant. Most of cyanobacteria were encrusted with the teardrop - or columnar shaped crystalline sheaths of copper minerals. FT-IR analyses, EPMA color mappings of carbon and TEM observations of the biomats demonstrated the biomineralization of copper minerals by microbial cell and extracellular sheaths. Cells and extracellular sheaths served the nucleation and deposition sites for ions and particles in solution. Microorganisms contributed in formation of copper minerals inside and outside of the cell, suggesting that microorganisms might alleviate copper toxicity.

## Stromatolite-like structure formations by cyanobacteria

Each cyanobacterial filament and cell changed into a nucleation site for copper mineralization and produced stromatolite-like structures. Formation of stromatolite-like structure occurred in two types: the banded structures in mm order and micro lamina. Banded structures formed by the differences such as cyanobacteria growth direction, distribution of cyanobacteria and mineral, and crystallinity. It was suggested that banded structures formed by seasonal change in growth direction and biomineralization rate of cyanobacteria. Additionally, the formation of micro lamina by cyanobacteria growing horizontally and vertically could be elucidated as follows:

*(1) Horizontal growth*

The horizontally cyanobacteria growth arranged parallel to the lamination. The thinnest laminae were composed of single cyanobacterial filaments, similar to that reported by Walter et al. (1976). The compositional lamination was also seen in this growth.

*(2) Vertical growth*

Numerous cyanobacteria grew towards to surface of biomats. The crystalline sheaths demonstrating micro lamination or colloform structure formed around cyanobacterial cells. One lamina or colloform structure was produced on each cell resulting in cyanobacterial filaments. Micro lamination was constructed by arrangement of these sheaths. This lamina which cyanobacterial cellular size was reflected was a minimum unit of stromatolite-like band.

## ACKNOWLEDGEMENTS

We would like to express our greatest gratitude to Prof. M. Akasaka of Shimane University, for his critical reading of the manuscript and valuable suggestions. We would thank Mr. T. Torigoe of Okayama Univversity, Mr. Y. Matsuda, Mr. S. Hatano and Mr. I. Yoshii for their cooperation to fieldwork and offer of the information for Dogamaru mine. We are also the most grateful for the members of Tazaki's Laboratory for their valuable discussions, very useful help and warm encouragement.

## REFERENCES

Akahane, H. and Yasuda, I. (1997) Precipitation of silica to the filamentous bacteria —Morphology of stromatolite in Nonphotosynthetic living body—. *J. Mineral. Soc. Japan*, **26**, 73-75.11.

Akai, K.and Akai, J. (1997) Manganese stromatolitic structure from Yunokoya hot spring. *J. Mineral. Soc. Japan*, **26**, 99-102.

Ashida, J., Higashi, N. and Kikuchi, T. (1963) An electronmicroscopic study on copper precipitation by copper-resistant yeast cells. *Protoplasma*, **57**, 27-32.

Banfield, J.F., Welch, S.A., Zhang, H., Ebert, T.T. and Penn, R.L. (2000) Aggregation-based crystal growth and microstructure development in natural iron oxyhydroxide biomineralization products. *Science*, **289**, 751-754.

Booth, G.H. and Mercer, S.J. (1963) Resistance to copper of some oxidizing and reducing bacteria. *Nature*, **199**, 622.

Chen, B.-Y., Utgikar, V.P., Harmon, S.M., Tabak, H.H., Bishop, D.F. and Govind, R. (2000) Studies on biosorption of zinc(II) and copper(II) on *Dsulfovibrio desulfuricans*. *Int. Biodeterioration & Biodegradation*, **46**, 11-18.

Cooksey, D.A. (1994) Molecular mechanisms of copper resistance and accumulation in bacteria. *FEMS Microbiol. Rev.*, **14**, 381-386.

Das, A., Modak, J.M. and Natarajan, K.A. (1997) Technical note studies on multi-metal ion tolerance of *Thiobacillus ferrooxidans*. *Mineral Engineering*, **10**, 743-749.

Deb, M., Banerjee, D.M. and Bhattacharya, A.K. (1978) Precambrian stromatolite and other structures in the Rajpura-Dariba polymetallic ore deposit, Rajasthan, India. *Mineral. Deposita*, **13**, 1-9.

Dönmez, G. and Aksu, Z. (1999) The effect of copper(Ⅱ) ions on the growth and bioaccumulation properties of some yeasts. *Process Biochemistry*, **35**, 135-142.

Ferris, F.G., Tazaki, K. and Fyfe, W.S. (1989) Iron oxides in acid mine drainage environments and their association with bacteria. *Chemical Geology*, **74**, 321-330.

Fowler, T.A. and Crundwell, F.K. (1998) Leaching of zinc sulfide by *Thiobacillus ferrooxidans*: experiments with a controlled redox potential indicate no direct bacterial mechanism. *Appl. Environ. Microbiol*, **64**, 3570-3575.

Freytet, P. and Verrecchia, E.P. (1998) Freshwater organisms that build stromatolites: a synopsis of biocrystallization by prokaryotic and eukaryotic algae. *Sedimentology*, **45**, 535-563.

Gadd G.M. (2000) Bioremedial potential of microbial mechanisms of metal mobilization and immobilization. *Environ. Biotech.*, **11**, 271-279.

Hata, A. (1997) Technology of metal industry and environmental pollution. Agune Gijutsu Center, 411p. Hudson-Edwards.

Hofmann, H.J. (2000) Archean stromatolites as microbial archives. *In* Riding, R.E. and Awramik, M., ed., *Microbial sediments*, Springer, 315-327.

Hudson-Edwards, K.A., Schell, C. and Macklin, M.G. (1999) Mineralogy and geochemistry of alluvium contaminated by metal mining in the Rio Tinto area, southwest Spain. *Appl. Geochem.*, **14**, 1015-1030.

Haynes, D.W. (1986) Stratiform copper deposits hosted by low-energy sediments: Ⅰ. Timing of sulfide precipitation —An hypothesis. *Econ. Geol.*, **81**, 250-265.

Holt, J.G., Krieg, N.R., Sneath, P.H.A., Staley, J.T. and Williams, S.T. (1994) Bergey's manual of determinative bacteriology ninth edition. Williams & Wilkins, 787p.

Humble, A.V., Gadd, G.M. and Codd, G.A. (1997) Binding of copper and zinc to three cyanobacterial microcystins quantified by differential pulse polarography. *Wat. Res.*, **31**, 1679-1686.

Iiyama, T. (1998) Introduction to the science of mineral resources. University of Tokyo Press, 195pp.

Kanno, K. and Fujii, H. (2000) Origin of the gross morphology and internal texture of tufas of Shimokawa Town, Ehime Prefecture, southwest Japan. *J. Geol. Soc. Japan*, **106**, 397-412.

Kikuchi, T. (1965) Some aspects of relationship between hyper-hydrogen sulfide-producing activity and

copper resistance of yeast. *Men. Coll. Sci. Univ. Kyoto, Ser. B*, **31**, 113-124.

Kishigami, Y., Sakurayama, K., Tazaki, K., Ueshima, M. and Watanabe, H. (1999) Bacterial fixation of Cu and Fe in Ogoya Mine, Ishikawa Prefecture. *Earth Sci.*, **53**, 19-28.

Kojima, S., Sudoh, R. and Chihara, M. (1995) Microorganism illustrated book. Kodansha, 758p.

Konhauser, K.O. and Urrutia, M.M. (1999) Bacterial clay authigenesis: a common biogeochemical process. *Chemical Geology*, **161**, 399-413.

Kotrba, P., Dolecková, L., Lorenzo, D.L. and Ruml, T. (1999) Enhanced bioaccumulation of heavy metal ions by bacterial cells due to surface display of short metal binding peptides. *Environ. Microbiol.*, **65**, 1092-1098.

Leblanc, M., Achard, B., Ben Othman, D., Luck, J.M., Bertrand-Sarfati, J. and Personné, J.Ch. (1996) Accumulation of arswnic from acidic mine waters by ferruginous bacterial accretions (stromatolites). *Appl. Geochem.*, **11**, 541-554.

Ledin, M. (2000) Accumulation of metals by microorganisms－processes and importance for soil systems. *Earth-Science Reviews*, **51**, 1-31.

Lippard, S.J. and Berg, J.M. (1994) Principles of bioinorganic chemistry. Tokyo Kagaku Dozin, 400pp.

Lippard, S.J. (1999) Free copper ions in the cell? *Science*, **30**, 748-749.

Little, B.J., Wagner, P.A. and Lewandowski, Z. (1997) Spatial relationships between bacteria and mineral surfaces. *In* Banfield, J.F. and Nealson, K.H., ed., *Reviews in mineralogy, volume 35, Geomicrobiology: Interactions between microbes and minerals*, Mineral. Soc. America, 123-159.

Livingstone, A. (1990) Copper-aluminium analogues of hydrohonessite and honessite, and woodwardite relationships. *Mineral. Mag.*, **54**, 649-653.

Lowe, D.R. (1994) Abiological origin of described stromatolites older than 3.2 Ga. *Geology*, **22**, 387-390.

Mann, H., Tazaki, K., Fyfe, W.S., Beveridge, T.J. and Humphrey, R. (1987) Cellular lepidocrocite precipitation and hevy-metal sorption in *Euglena* sp. (unicellular algae): implications for biomineralization. *Chemical Geology*, **63**, 39-43.

Martin, J.-M. and Meybeck, M. (1979) Elemental mass-balance of material carried by major world rivers. *Marine Chem.*, **7**, 173-206.

Matsuda, T. and Oda, M. (1982) Geology of the late Cretaceous to Paleogene igneous rocks in the Kawamoto area Shimane Prefecture, Southwest Japan. *J. Geol. Soc. Japan*, **88**, 31-42.

Matsuda, Y. and Akasaka, M. (1995) Ore minerals in Dogamaru mine, Shimane Prefecture, Japan. *The Society of Resource Geology, the Japanese Association of Mineralogists, Petrologists and Economic Geologists, the Mineralogical Society of Japan Joint Annual Meeting Abstracts with Programs*, 129.

McNeil, M.B., Jones, J.M. and Little, B.J. (1991) Production of sulfide minerals by sulfate-reducing bacteria during microbiologically influenced collosion of copper. *Corrosion*, **47**, 674-677.

Mejáre, M. and Bülow, L. (2001) Metal-binding proteins and peptides in bioremediation and phytoremediation of heavy metals. *Trends Biotechnol.*, **19**, 67-73.

Mendelsohn, F. (1976) Mineral deposits associated with stromatolites. *In* Walter, M.R., ed., *Developments in Sedimentology 20 Stromatolites*, Elsevier Scientific Publishing Company, Amsterdam, 645-662.

Monty, C.L.V. (1976) The origin and development of cryptalgal fabrics. *In* Walter, M.R., ed., *Developments in Sedimentology 20 Stromatolites*, Elsevier Scientific Publishing Company, Amsterdam, 193-259.

Morsi Abd-El-Monem, H., Corradi, M.G. and Gorbi, G. (1998) Toxicity of copper and zinc to two strains of Scenedesmus acutus having different sensivity to chromium. *Environ. Exp. Bot.*, **40**, 59-66.

Nickel, E.H. (1976) New data on woodwardite. *Mineral. Mag.*, **43**, 644-647.

Narita, E. (2001) Interaction between anionic clays and organic compounds. *Clay Sci.*, **40**, 173-178.

Nishioka, G.K., Kelly, W.C. and Elmore, R.D. (1984) Copper occurrences in stromatolites of the Copper Harbor Conglomerate, Keweenaw Peninsula, northern Michigan. *Econ. Geol.*, **79**, 1393-1399.

Omori, T, Nojiri, H., Horinouchi, M. and Kasuga, K. (2000) Environmental Biotechnology. Shoko-do, 190p.

Panchanadikar, V.V. and Das, R.P. (1993) Biorecovery of zinc from industrial effluent using native microflora. *Intern. J. Environ. Stud.*, **44**, 251-257.

Pope, M.C., Grotzinger, J.P. and Schreiber, B.C. (2000) Evaporitic subtidal stromatolites produced by *in situ* precipitation: textures, facies associations, and temporal significance. *J. Sedimentary Research*, **70**, 1139-1151.

Preidl, M. and Metzler, M. (1984) The sedimentation of copper-bearing shales (Kupferschiefer). *Mineral Deposita*, **19**, 243-248.

Raade, G., Elliott, C.J. and Din, V.K. (1985) New data on glaucocerinite. *Mineral. Mag.*, **49**, 583-590.

Renaut, R.W., Jones, B. and Tiergelin, J.J. (1998) Rapid *in situ* silicification of microbes at Loburu hot springs, Lake Bogoria, Kenya Rift Valley. *Sedimentology*, **45**, 1083-1103.

Reserch Group for the San'in Late Mesozoic Igneous Activity (1979) Late Cretaceous to Paleogene igneous rocks in the Ouchi district, central Shimane prefecture, western Honshu. *The memoires of the Geol. Soc. Japan*, **17**, 249-258.

Rose A.W. and Bianchi-Mosquera, G.C. (1993) Adsorption of Cu, Pb, Zn, Co, Ni and Ag on Goethite and Hematite: A control on metal mobilization from red beds into stratiform copper deposits. *Econ. Geol.*, **88**, 1226-1236.

Sánchez, A., Ballester, A., Blázquez, M. L., González, F., Muñoz, J. and Hammaini, A. (1999) Biosorption of copper and zinc by *Cymodocea nodosa*. *FEMS Microbiol. Rev.*, **23**, 527-536.

Seong-joo, L., Browne, K.M. and Golubic, S. (2000) On stromatolite lamination. *In* Riding, R.E. and Awramik, S.M., ed., *Microbial sediments*, Springer-Verlag, 16-24.

Shikaura, H. and Tazaki, K. (2001) Cementations of sand grains are accelerated by microbes －formation of bio-terrace at Satsuma Iwo-Jima Island－. *clay sci.*, **40**, 229-241.

Shimane Prefecture (1985) Geology of Shimane Prefecture, The Shimane Pref. Geol. Mapping Committee, 451-452pp.

Silver, S. (1997) The bacterial view of the periodic table: specific functions for all elements. *In* Banfield, J.F. and Nealson, K.H., ed., *Reviews in mineralogy, volume 35, Geomicrobiology: Interactions between microbes and minerals*, Mineral. Soc. America, 345-360.

Sze, K. F., Lu, Y.J. and Wong, P.K. (1996) Removal and recovery of copper ion ($Cu^{2+}$) from electroplating

effluent by bioreactor containing magnetite-immobilized cells of *Pseudomonas putida* 5X. *Resources, Conservation and Recycling*, **18**, 175-193.

Takada, M. and Matsuuchi, S. (1981) Secondary minerals from the Kabasaka mine & Nyukaku mine, Hyogo Pref. —Serpierite・Devilline・Langite・Spangolite & Woodwardite—. *Chigaku Kenkyu*, **32**, 7-12.

Takamura, N., Kasai, F. and Watanabe, M.M. (1989) Effects of Cu and Zn photosynthesis of fresh water benthic algae. *J. Appl. Phycol.*, **1**, 39-52.

Tashiro, Y. and Tazaki, K. (1999) The primitive stage of microbial mats comprizing iron hydroxides. *Earth Sci.*, **53**, 29-37.

Tazaki, K., Ishida, H., Moriyama, K. and Mori, T. (1992) The accumulation of heavy metals in the activated sludge by bacteria —observation and analysis with electron microscope—. *Environ. Sci.*, **5**, 57-66.

Tazaki, K. (1997) Microbial mats in Japan -Microbial biomineralization-. Knazawa Univ., 91p.

Tazaki, K. (1999) Architecture of biomats reveals history of geo-, aqua-, and bio-systems, *Episodes*, **22**, 21-25.

Tazaki, K. (2000) Formation of banded iron-manganese structures by natural microbial communities, *Clays and Clay Minerals*, **48**, 511-520.

Tazaki, K., Islam, ABM. R., Nagai, K. and Kurihara, T. (2002) $FeAs_2$ biomineralization on encrusted bacteria in hot springs: An ecological role of symbiotic bacteria. *Canadian Journal of Earth Science* (submited).

Temple, K.L. and Le Roux, N.W. (1964) Syngenesis of sulfide ores: sulfate-reducing bacteria and copper toxicity. *Econ. Geol.*, **59**, 271-278.

Ueshima, M. and Tazaki, K. (2001) Possible role of microbial polysaccharides in nontronite formation. *Clays and Clay Minerals*, **49**, 292-299.

Walter, M.R. (1976) Developments in Sedimentology 20 Stromatolites. Walter, M.R., ed., Elsevier Scientific Publishing Company, Amsterdam, 790p.

Walter, M.R., Bauld, J. and Brock, T.D. (1976) Microbiology and morphogenesis of columnar stromatolites (Conophyton, Vacerrilla) from hot springs in Yellowstone National Park. *In* Walter, M.R., ed., *Developments in Sedimentology 20 Stromatolites*, Elsevier Scientific Publishing Company, Amsterdam, 273-310.

Wang, T.C., Weissman, J.C., Ramesh, G., Varadarajan, R. and Benemann, R. (1998) Heavy metal binding and removal by *Phormidium*. *Bull. Environ. Contam. Toxicol*, **60**, 739-744.

Watanabe, H. and Tazaki, K. (1998a) Biomats formed in copper mine drainage. *The Joint Meeting of Earth and Planetary Science Abstracts*, 188.

Watanabe, H. and Tazaki, K. (1998b) Biomats formed in the copper mine drainage. *International Mineralogical Association 17th General Meeting, Abstracts & Programe*, A75.

Watanabe, H. and Tazaki, K. (1999) Formation of copper bed by microorganisms. *The Clay Science Society of Japan 43th Annual Meeting Abstracts*, **43**, 218-219.

Watanabe, H. and Tazaki, K. (2000) Woodwardite formed in biomats in copper mine drainages. *The 107th*

*Annual Meeting of the Geol. Soc. Japan Abstracts*, 215.

Watanabe, M., Harada, K. and Fujiki, H. (1994) Waterbloom of blue-green algae and their toxins. University of Tokyo Press, 257p.

Witzke, T. (1993) Neufunde aus Sachsen: Spangolith, Namuwit, Schulenbergit, Woodwardite und Parnauit. *Lapis*, **12**, 15-18.

Witzke, T. (1999) Hydrowoodwardite, a new mineral of the hydrotalcite group from Konigswalde near Annaberg, Saxony/Gemany and other localities. *N. Jb. Miner. Mh.*, **2**, 75-86.

Yamamoto, H., Tatsuyama, K. and Uchiwa, T. (1985) Fungal flora of soil polluted with copper. *Soil Biol. Biochem.*, **17**, 785-790.

Yasuda, T., Katoh, H. and Tazaki, K. (2000) Crystal growth of calcite in microbial mats in hot springs is controlled by microorganisms. *Jour. Geol. Soc. Japan*, **106**, 548-559.